Instrument for the Identification of Live and Dead Bacteria

Arjun Krishnamoorthi

SUBSYSTEM REPORTS

REVISION – Original
4 December 2019

SUBSYSTEMS REPORT
FOR
Instrument for the Identification of Live and Dead Bacteria

TEAM <52>

APPROVED BY:

_____
Arjun Krishnamoorthi Date

_____
John Lusher II, P.E. Date

_____
T/A Date

Change Record

Rev.	Date	Originator	Approvals	Description
1	12/4/2019	Arjun Krishnamoorthi		Original Release

Table of Contents

List of Tables

List of Figures

1. Introduction

The portable fluorescence spectrometer will be capable of recording the normal fluorescence and synchronous fluorescence spectra of bacteria, in addition to performing ultraviolet (UV) disinfection on bacterial samples *in-situ*. The fluorescence spectra of bacteria, before and after UV disinfection, will be recorded and processed through principal component analysis (PCA) as a means of rapidly distinguishing live and dead bacteria. A GUI will support the acquisition, processing, and display of spectral data. To that effect, the portable fluorescence spectrometer is composed of four subsystems: (1) a control and display unit, (2) a disinfection unit, (3) an excitation monochromator, and (4) an emission monochromator. All subsystems were successfully designed, constructed, and validated.

2. Control and Display Unit Subsystem Report

2.1. Subsystem Introduction

The main purpose of the control and display unit subsystem is to receive inputs from the user, communicate with both the excitation monochromator and emission monochromator subsystems, and process and display recorded spectral data. Relevant inputs from the user include (1) the type of spectrum (normal fluorescence or synchronous fluorescence) to record, (2) acquisition parameters (e.g., exposure time, number of spectra to record, etc.), and (3) PCA processing details, among others. Communication with the excitation monochromator subsystem consists of rotating the excitation grating, while communication with the emission monochromator subsystem consists of interfacing with the linear image sensor, setting acquisition parameters, and subsequently reading fluorescence spectra. Finally, once spectral data is successfully recorded, displayed, and stored, PCA and other data processing, such as median filtering, may be performed as well.

2.2. Subsystem Details

2.2.1. MATLAB GUIs and Laptop

The current embodiment of the control and display unit subsystem is a compact laptop (Dell Precision 5510 Mobile Workstation Laptop) executing custom MATLAB software. The software currently consists of two independent GUIs; one is an acquisition GUI for communicating with the excitation and emission monochromators, while the other is a processing GUI for performing PCA on recorded spectral data. These GUIs were designed through the App Designer feature of MATLAB to simplify the actual creation of the GUI layout and its various buttons, text fields, and checkboxes. To that effect, the majority of programming done for the GUI itself involved implementing various callbacks. The acquisition GUI and processing GUI are shown in Figure 1 and Figure 2, respectively, on the following page.

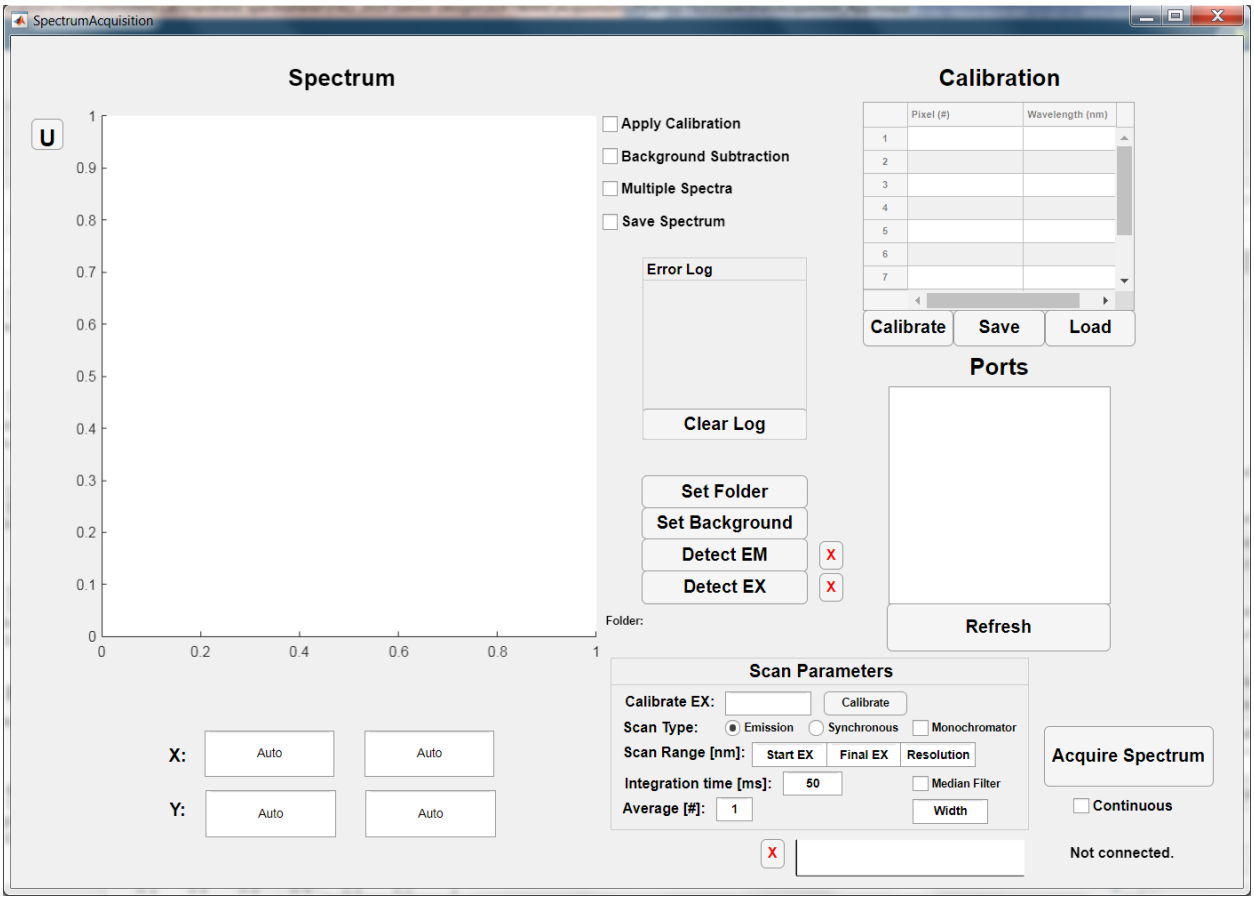

Figure 1: MATLAB acquisition GUI for communicating with excitation monochromator and emission monochromator subsystems.

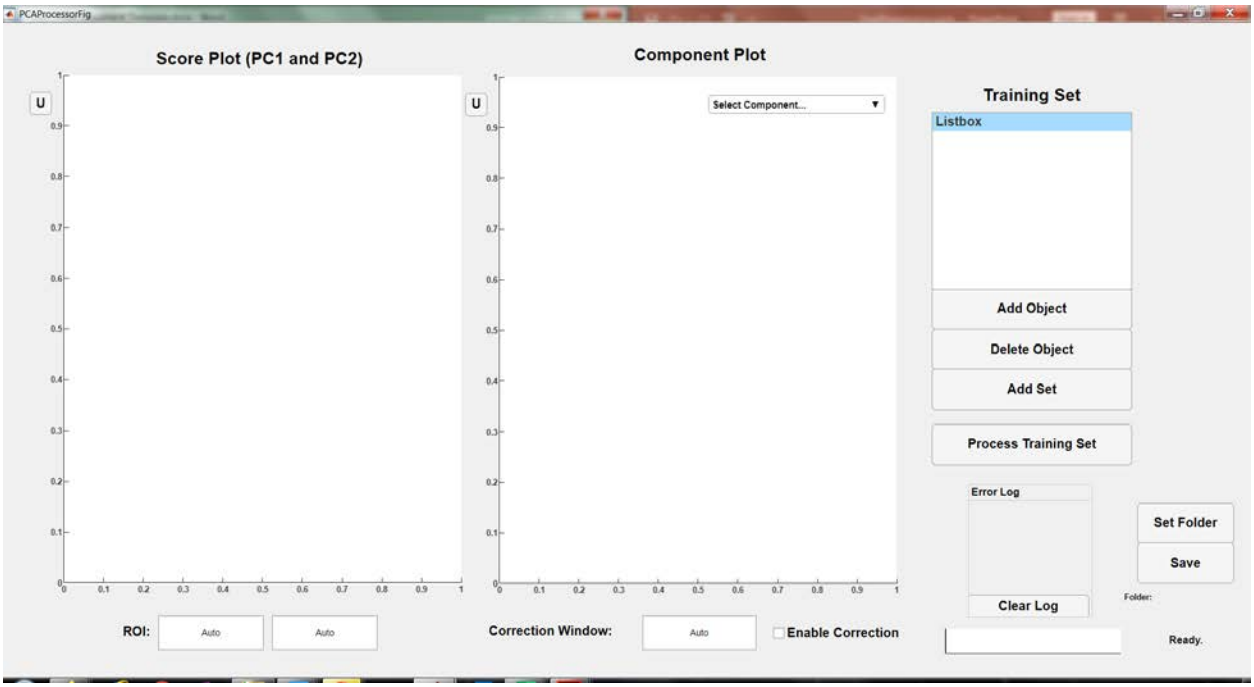

Figure 2: MATLAB processing GUI for performing and optimizing PCA on recorded data.

A variety of functionalities are currently available in the acquisition GUI, including the ability to record both normal fluorescence and synchronous fluorescence spectra, alter acquisition parameters, save spectra, calibrate the spectrometer and excitation monochromator, and perform background subtraction. In the processing GUI, the user may perform PCA on recorded spectral data and view the associated score and component plots. In addition, the user may also fine-tune the PCA processing by adjusting the region of interest (ROI), which essentially represents the range of fluorescence data subjected to PCA, or performing median filtering on the data to reduce noise and improve clustering.

Communication with the excitation and emission monochromator subsystems is achieved through a common serial communication link which allows commands to be issued to both subsystems simultaneously through separate serial ports. Namely, one serial cable connects to an RS-232 communication port integrated with the emission monochromator subsystem, while another serial cable feeds into the serial port of the microcontroller within the excitation monochromator subsystem. Figure 3 shows the basic functional block diagram (FBD) of this setup, while Figure 4 is a picture of its implementation.

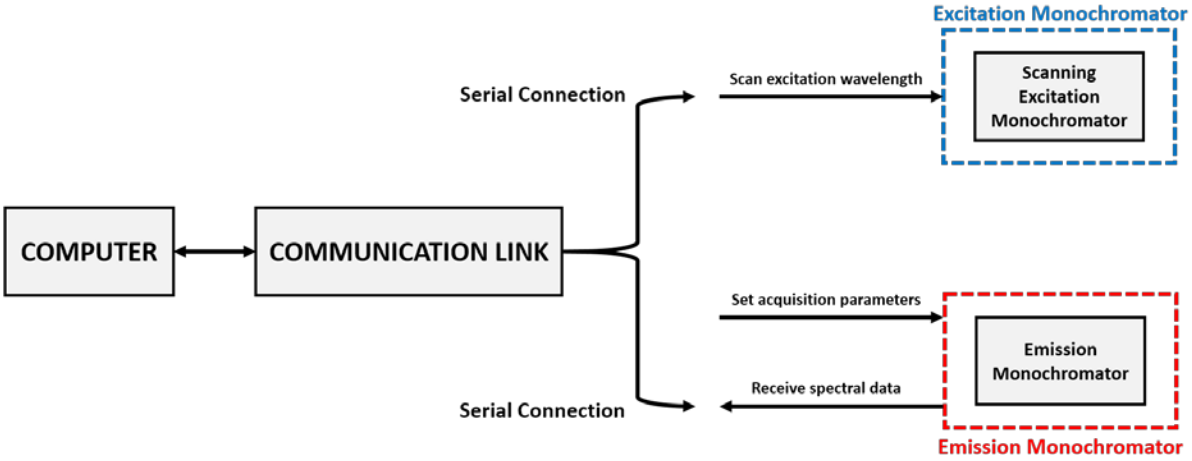

Figure 3: FBD for serial connection between computer and excitation monochromator and emission monochromator subsystems.

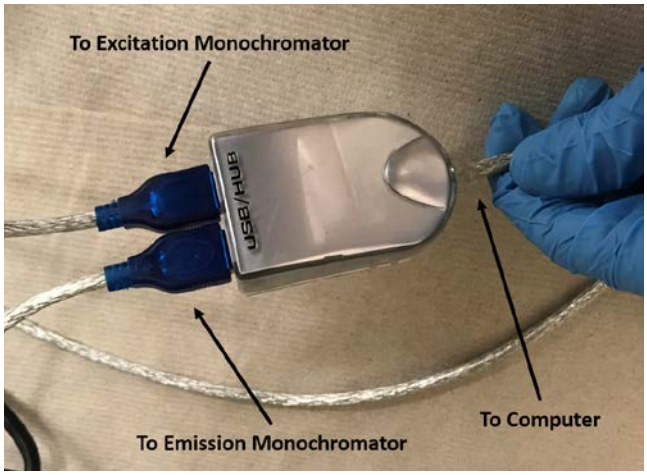

Figure 4: Implementation of serial connection between computer and excitation monochromator and emission monochromator subsystems.

To achieve communication with both subsystems simultaneously, individual serial port connections need to be established in MATLAB. The configuration of these serial port connections (e.g., baud rate, parity, data bit, etc.) was determined by the respective communication protocols associated with each subsystem.

2.2.2. Excitation Monochromator Subsystem Communication

Communication with the excitation monochromator subsystem is achieved through the serial port of the microcontroller within the subsystem. The microcontroller is a DCB-241, which is an integrated stepper motor driver-controller board that operates on an RS-422 communication protocol. To simplify the software development, a SIN-11 intelligent serial adapter, shown in Figure 5, was utilized as a means of converting the RS-232 bus from the computer into an RS-422 bus. The overall communication setup is shown in Figure 6. Furthermore, details concerning the serial port configuration for this communication are noted in Table 1 below.

Figure 5: SIN-11 intelligent serial adapter for converting RS-232 bus into an RS-422 bus for communication with the DCB-241 microcontroller.

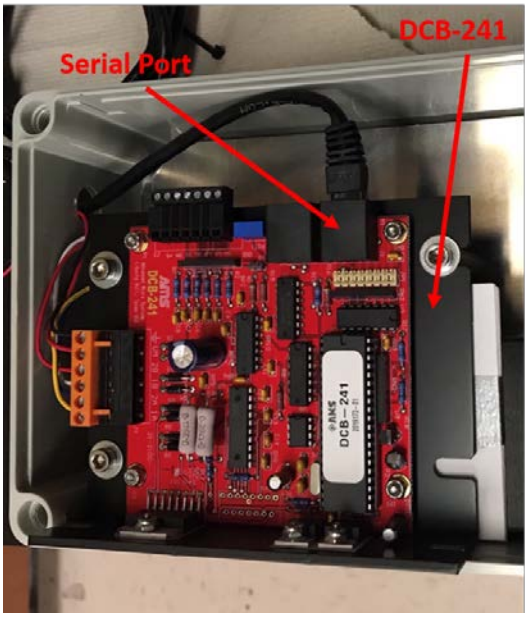

Figure 6: Overall communication setup for excitation monochromator subsystem, including the DCB-241 and its serial port.

Specification	Value
Baud Rate (bps)	9600
Data Bits	8
Stop Bits	1
Parity	None
Flow Control	Hardware
Handshaking	None

Table 1: Serial port configuration for excitation monochromator subsystem [1].

The primary purpose of the DCB-241 microcontroller is to rotate the excitation grating within the excitation monochromator subsystem by means of a stepper motor. To that effect, the serial port connection with the subsystem is utilized as a means of issuing high-level, ASCII commands for configuring and initiating the rotation of the stepper motor. A table of the most relevant commands is provided in Table 2 on the following page. The full set of commands is available in the associated DCB-241 documentation [1].

Command	Function	Value	Notes
I	Initial Velocity	18-23,000 SPS	The initial velocity specifies the start and stop speed, in steps per second (SPS), for the motor.
K	Ramp Slope	0-255	The ramp slope specifies the ramp acceleration and deceleration time.
V	Slew Velocity	18-23,000 SPS	The slew velocity is the final velocity following acceleration from the initial velocity.
+	Index in Plus Direction	0-16,777,215 Steps	This command steps the stepper motor in a positive direction for the specified number of steps.
-	Index in Minus Direction	0-16,777,215 Steps	This command steps the

			stepper motor in a negative direction for the specified number of steps.
S	Store Parameters	N/A	This command saves all operational parameters for recall during power-on reset.

Table 2: Relevant DCB-241 commands for rotating the stepper motor [1].

2.2.3. Emission Monochromator Subsystem Communication

Communication with the emission monochromator subsystem is achieved through an RS-232 port integrated with the onboard control electronics. The emission monochromator is an off-the-shelf BTC110-S spectrometer from B&W TEK. Owing to the onboard RS-232 port, a serial cable, shown in Figure 6, may be directly connected from the computer to the subsystem for communication. Details concerning the serial port configuration for this communication are noted in Table 3 below.

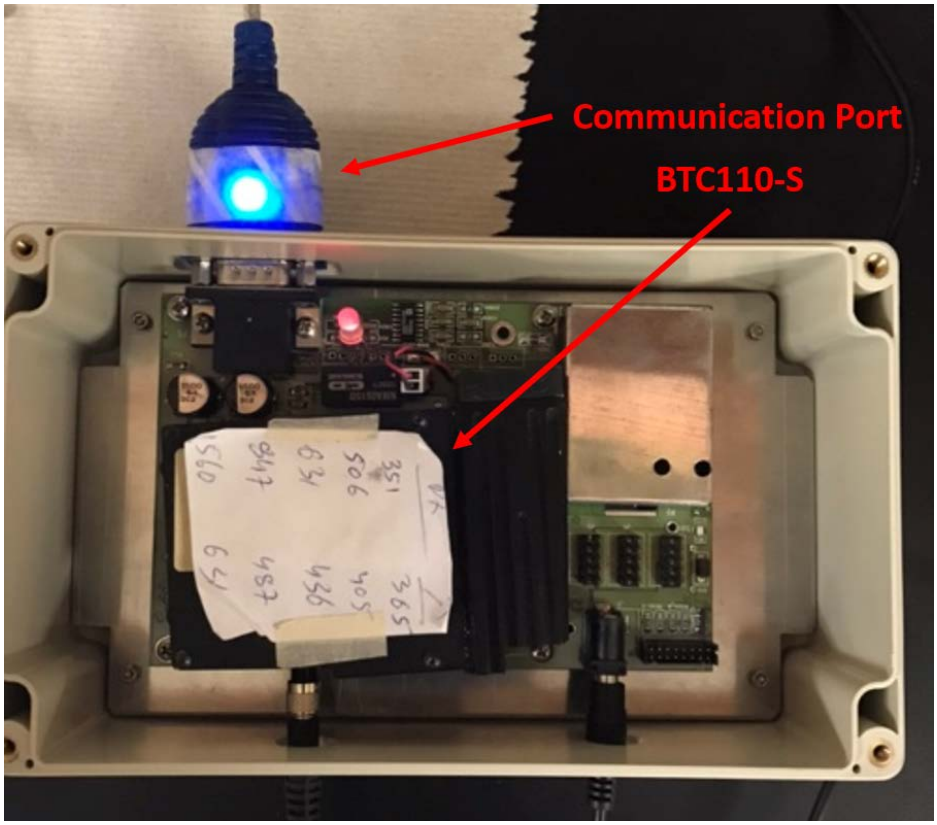

Figure 7: Overall communication setup for emission monochromator subsystem, including the BTC110-S and its serial port.

Specification	Value
Baud Rate (bps)	9600
Data Bits	8
Stop Bits	1
Parity	None
Flow Control	Hardware
Handshaking	None

Table 3: Serial port configuration for emission monochromator subsystem [2].

The primary purpose of the BTC110-S spectrometer is to detect, digitize, and record the fluorescence spectra of bacterial samples. To that effect, the serial port connection with the subsystem is utilized as a means of issuing high-level, ASCII commands for configuring acquisition parameters (e.g., integration time, averaging, etc.) and receiving spectral data from the linear image sensor within the optical bench. A table of the most relevant commands is provided in Table 4 below. The full set of commands is available in the associated BTC110-S documentation [2].

Command	Function	Value	Notes
K	Set Baud Rate	0	This command can be used to increase the baud rate (bps) to as high as 115,200 bps.
I	Set Integration Time	50-65535	This command can be used to set the integration time (milliseconds).
A	Set Averaging	1-1000000000	This command can be used to set the number of spectra to average in a given spectrum acquisition.
a	Set ASCII Mode	N/A	This command switches the communication into ASCII mode.
b	Set Binary Mode	N/A	This command switches the communication into binary mode.

?K	Query Baud Rate	N/A	This command queries the current baud rate (bps).
?I	Query Integration Time	N/A	This command queries the current integration time (milliseconds).
?A	Query Averaging	N/A	This command queries the current number of spectra to be averaged.
?a	Query Communication Mode	N/A	This command queries the current communication mode (ASCII or binary).

Table 4: Relevant BTC-110S commands for configuring and reading the spectrometer [2].

2.2.4. Acquiring Normal Fluorescence Spectra

Normal fluorescence spectra describe the fluorescence of bacteria at a fixed, constant excitation wavelength λ_{EX}. This data is recorded by utilizing either the disinfection unit or excitation monochromator as a fixed excitation source and subsequently measuring the fluorescence of the bacterial sample through the emission monochromator subsystem. Briefly, this process requires identifying the excitation source (i.e., disinfection unit or excitation monochromator), configuring acquisition parameters, acquiring spectral data, processing the data, and outputting the data through a MATLAB figure and CSV file. The control logic for this process is detailed in Figure 8 on the subsequent page. It is worthy to mention that the excitation intensity of the disinfection unit at the sample location is much higher compared to that of the excitation monochromator. Therefore, for normal fluorescence measurements, it is preferable to utilize solely the disinfection unit.

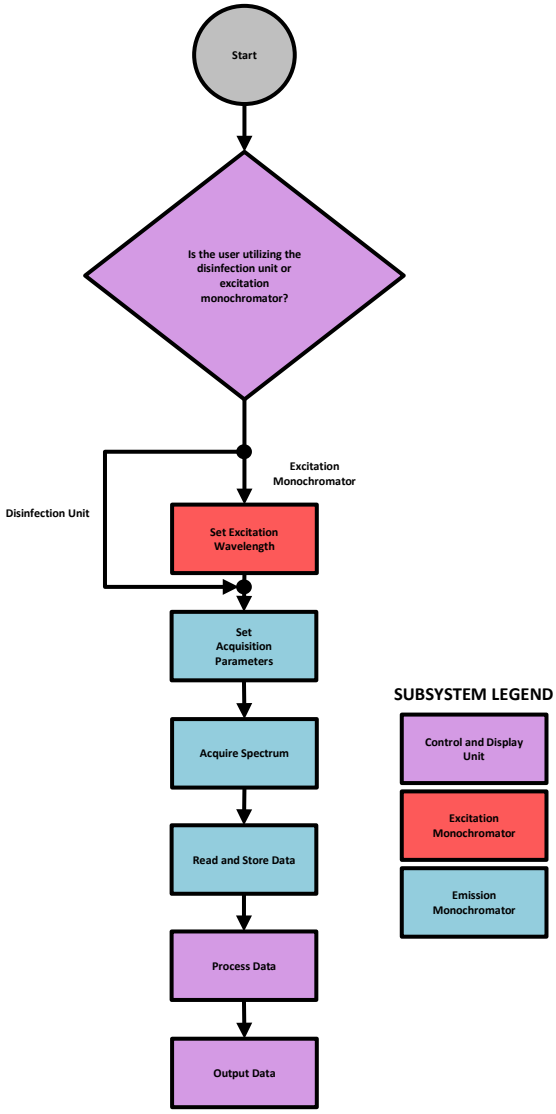

Figure 8: System flowchart detailing the normal fluorescence measurement.

2.2.5. Acquiring the Excitation-Emission Matrix (EEM)

An Excitation-Emission Matrix (EEM) is a three-dimensional dataset which consists of a sample's fluorescence spectra across a set of excitation wavelengths. The EEM can offer a complete, detailed characterization of the fluorescence from an unknown sample. This data is recorded by utilizing the excitation monochromator as a scanning excitation source and subsequently measuring the fluorescence of the bacterial sample over a range of excitation wavelengths. Briefly, this process requires calibrating and configuring the excitation monochromator, configuring acquisition parameters, acquiring spectral data over a range of scanned excitation wavelengths, processing the data, and outputting the data through a MATLAB figure and CSV file. The EEM may be provided as either a three-dimensional (3D)

surface plot or two-dimensional (2D) contour plot. The control logic for this process is detailed in Figure 9 below.

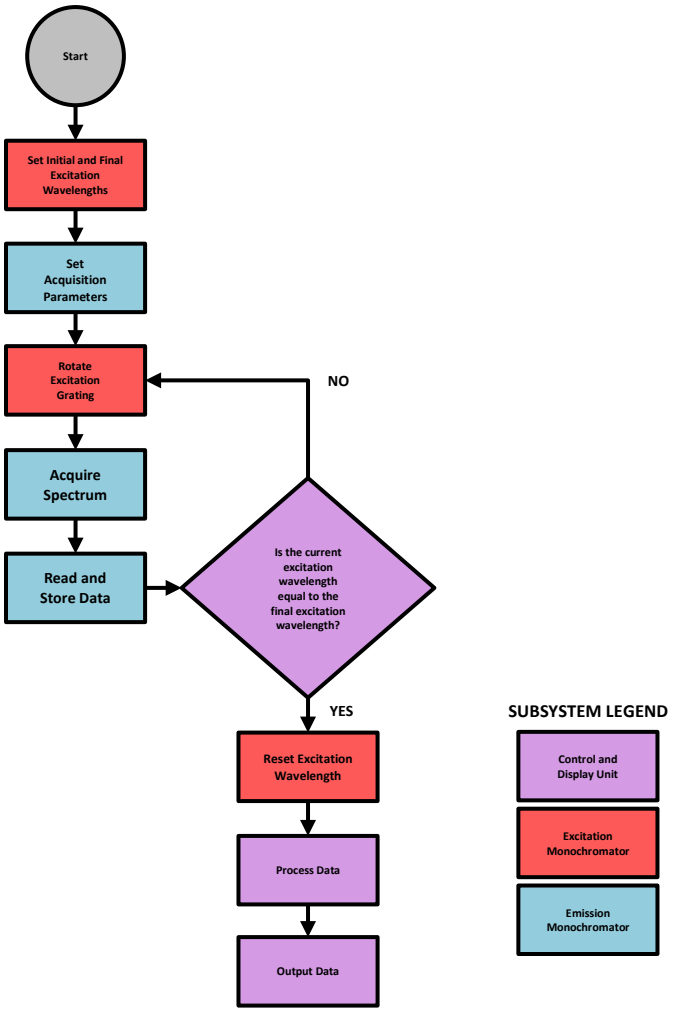

Figure 9: System flowchart detailing the EEM measurement.

2.2.6. Acquiring Synchronous Fluorescence Spectra

Synchronous fluorescence spectra are a particular type of fluorescence spectra which can resolve the fluorescence of individual components in a mixture or multicomponent sample [3]. With bacteria, synchronous fluorescence is an especially useful technique for resolving the fluorescence of its cellular components, namely tryptophan and tyrosine. To that effect, this technique can offer more detailed information on a molecular level than normal fluorescence. In commercial, benchtop spectrometers, this technique is generally achieved by synchronously scanning both the excitation monochromator and emission monochromator such that the excitation wavelength, λ_{EX}, and emission wavelength, λ_{EM}, satisfy the following relation:

$$\Delta\lambda = \lambda_{EM} - \lambda_{EX}.$$

$\Delta\lambda$ is a quantity which denotes the constant offset in wavelength maintained between the monochromators. This quantity is a rather critical parameter in determining which fluorescence bands are resolved in a mixture. Alternatively, synchronous fluorescence spectra may simply be extracted from a sample's EEM by considering the fact that the relation $\lambda_{EM} = \lambda_{EX} + \Delta\lambda$ is simply a linear equation with a slope equal to unity and intercept equal to $\Delta\lambda$. Synchronous fluorescence spectra may therefore be simply interpreted as a set of parallel lines with varying intercepts that exist within a sample's EEM. To that end, once an EEM is acquired, synchronous fluorescence spectra of varying $\Delta\lambda$ may be efficiently acquired within the software itself. Currently, once a bacterial EEM is acquired, synchronous spectra across a range of $\Delta\lambda$ are automatically extracted and written to a separate CSV file.

2.3. Subsystem Validation

2.3.1. Acquisition GUI

The validation of the acquisition GUI was performed through validation of the excitation monochromator and emission monochromator subsystem communication itself. Alongside, functionalities such as the ability to save spectra, calibrate the spectrometer, and perform background subtraction, among others, were thoroughly tested by performing experiments on bacterial samples. Many of these experimental results will be provided in the subsystem reports for the excitation monochromator and emission monochromator subsystems. Debugging and further development of this GUI will continue into next semester.

The normal fluorescence, excitation-emission matrix (EEM), and synchronous fluorescence of *E. coli* bacteria are provided on the subsequent pages to illustrate typical outputs of the acquisition GUI. Outputs are generated as both MATLAB figures and CSV files to simplify plotting of the data.

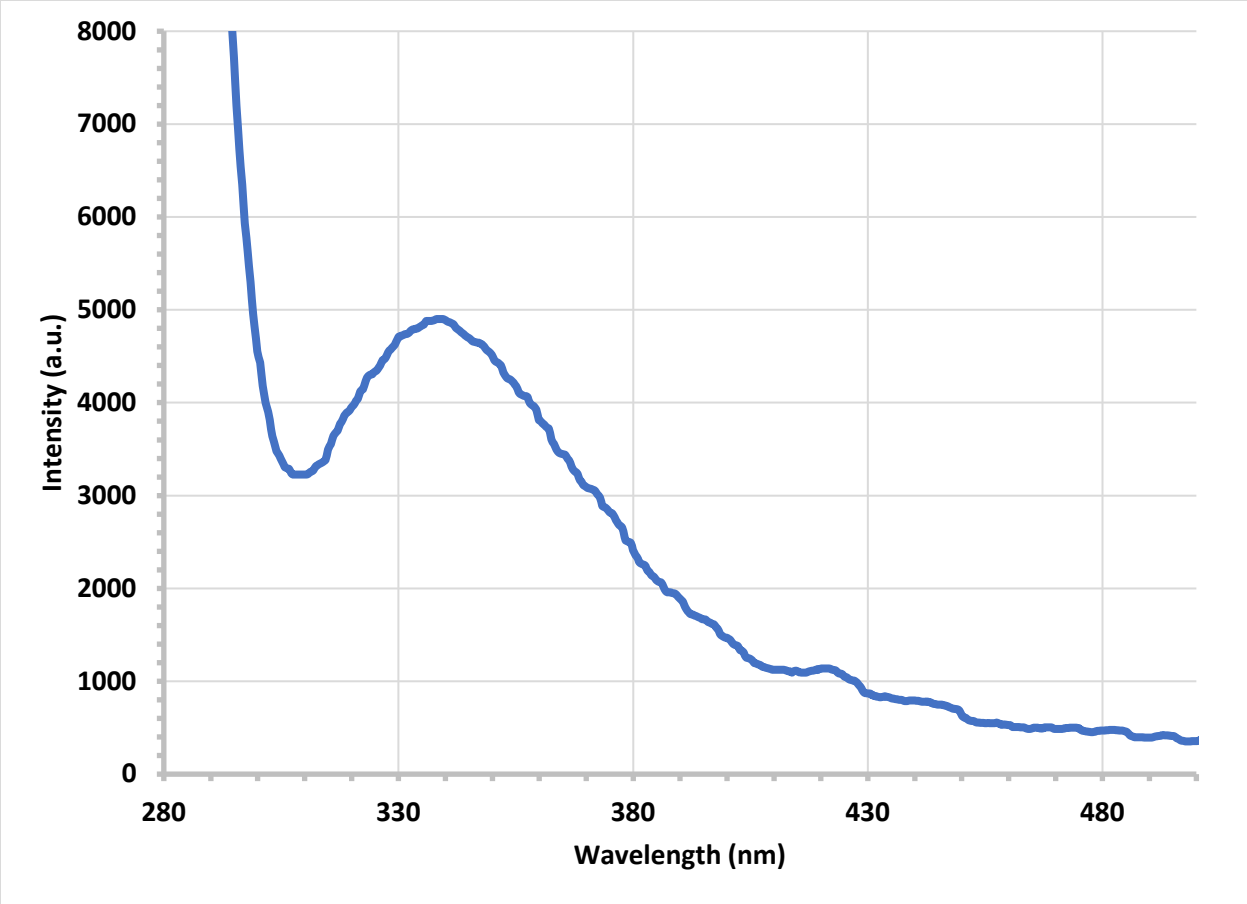

Figure 10: Normal fluorescence ($\lambda_{EX} \approx 285$ nm) spectrum of *E. coli* bacteria ($\approx 10^8$ cells/mL).

Figure 10 is a plot of the normal fluorescence spectrum of *E. coli*. The vertical axis is the fluorescence intensity, while the horizontal axis is the emission wavelength. This spectrum was acquired with the disinfection unit as the fixed excitation source. The initially high intensity is due to Rayleigh (elastic) scattering of the excitation beam. The fluorescence band of *E. coli* is clearly observed with a maximum at approximately 340 nm. This fluorescence is due, primarily, to tryptophan and tyrosine residues within the bacterial cells. Because the excitation wavelength is fixed, we are unable to resolve the fluorescence of tryptophan and tyrosine individually. The validation of this measurement is provided in the emission monochromator and excitation monochromator subsystem reports.

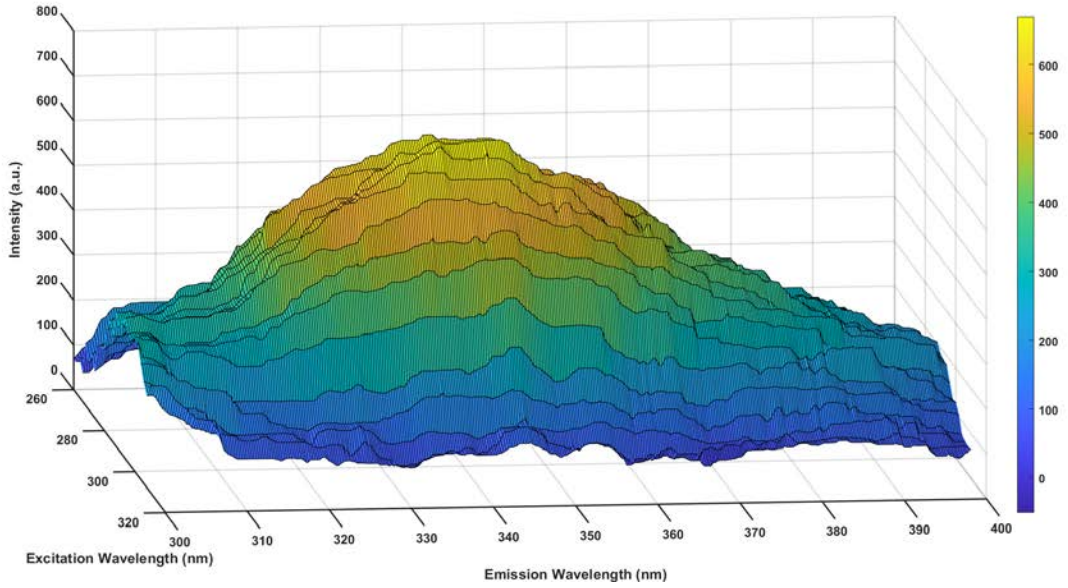

Figure 11: 3D surface plot of EEM for *E. coli* bacteria (≈ 10^8 cells/mL) acquired over an excitation range of 260 to 310 nm in 2 nm steps.

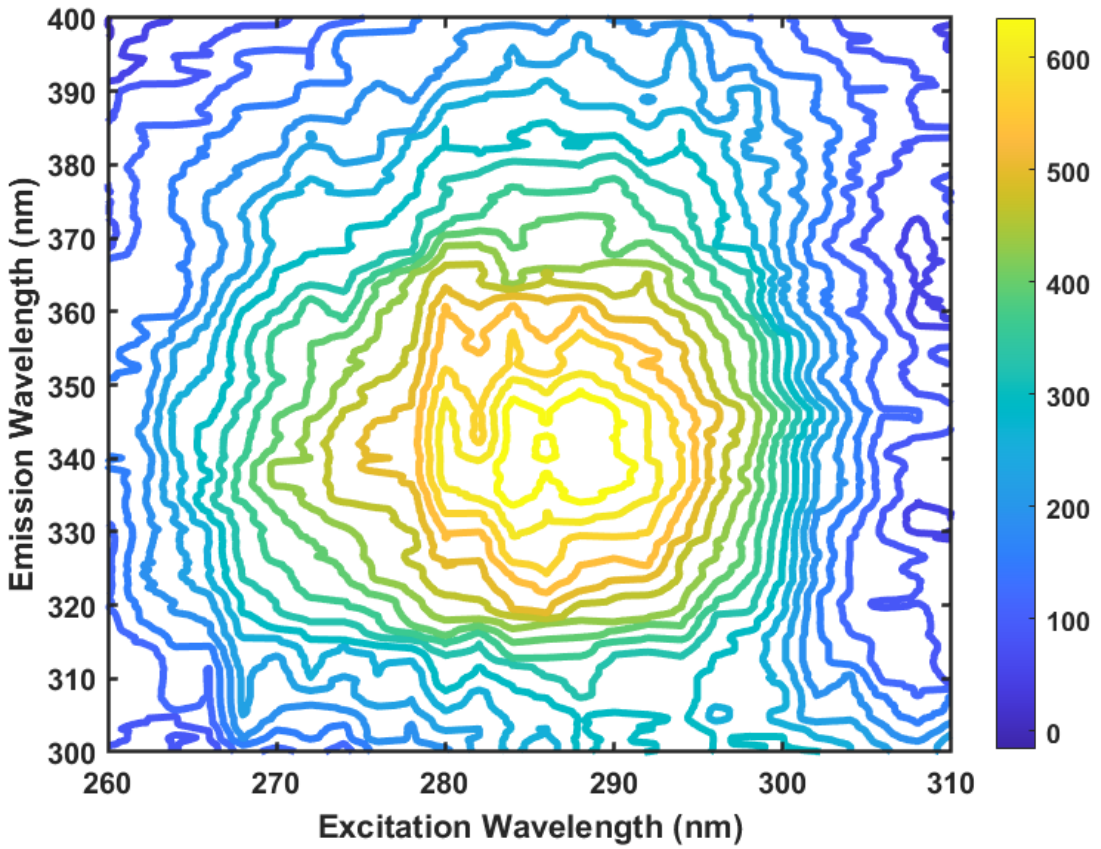

Figure 12: 2D contour plot of EEM for *E. coli* bacteria (≈ 10^8 cells/mL) acquired over an excitation range of 260 to 310 nm in 2 nm steps.

The EEM shown in Figure 11 and Figure 12 was acquired across an excitation range of 260 to 310 nm in 2 nm steps with the excitation monochromator as a scanning excitation source. Clearly, the EEM offers a complete, detailed characterization of the fluorescence bands of *E. coli*. From this EEM, we may extract the synchronous spectra of the tryptophan and tyrosine components in *E. coli*.

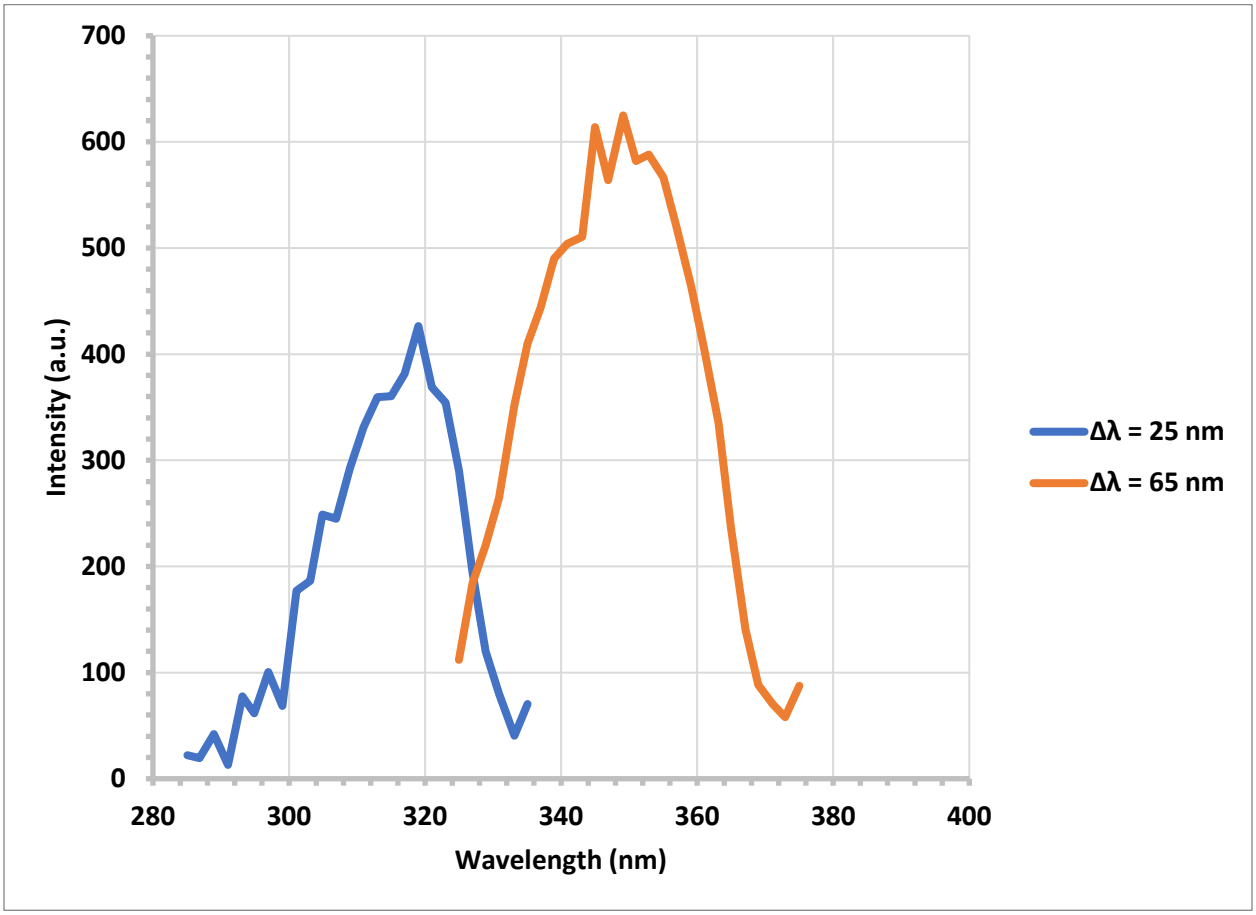

Figure 13: Synchronous fluorescence spectra ($\Delta\lambda = 25$ nm and $\Delta\lambda = 65$ nm) of *E. coli* bacteria ($\approx 10^8$ cells/mL).

Figure 13 is a plot of the synchronous fluorescence spectra of *E. coli* at $\Delta\lambda = 25$ nm and $\Delta\lambda = 65$ nm, which correspond, respectively, to the tyrosine and tryptophan components within the bacterial cells. These synchronous fluorescence spectra were extracted from the EEM shown in Figure 11 and Figure 12. The EEM and synchronous fluorescence spectra thus provide a means of resolving the fluorescence of individual components within bacterial cells. The validation of the EEM and synchronous fluorescence measurements is provided in the emission monochromator and excitation monochromator subsystem reports.

2.3.2. Processing GUI

The validation of the processing GUI was performed through the generation of PCA score and component plots for experimental data recorded through the acquisition GUI. Alongside, functionalities such as the ability to tune the ROI, perform median filtering, and save PCA results were thoroughly tested. Many of these PCA results will be provided in the subsystem reports for the excitation monochromator and emission monochromator subsystems. Debugging and further development of this GUI will continue into next semester.

PCA score and component plots for experimental data are provided below and on the subsequent page to illustrate typical outputs of the processing GUI. Outputs are generated as both MATLAB figures and CSV files to simplify plotting of the data.

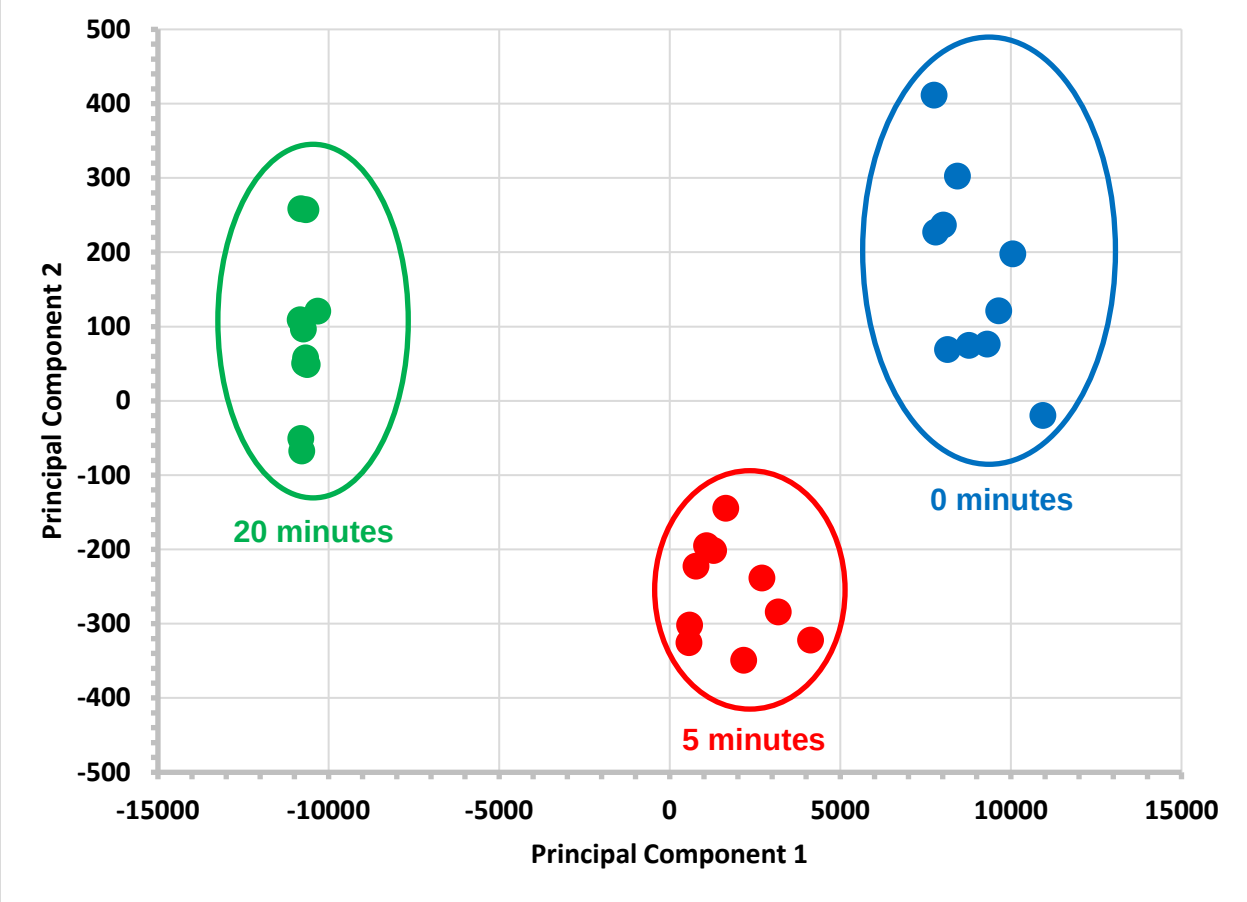

Figure 14: PCA score plot for UV irradiation experiment on *E. coli* bacteria ($\approx 10^8$ cells/mL).

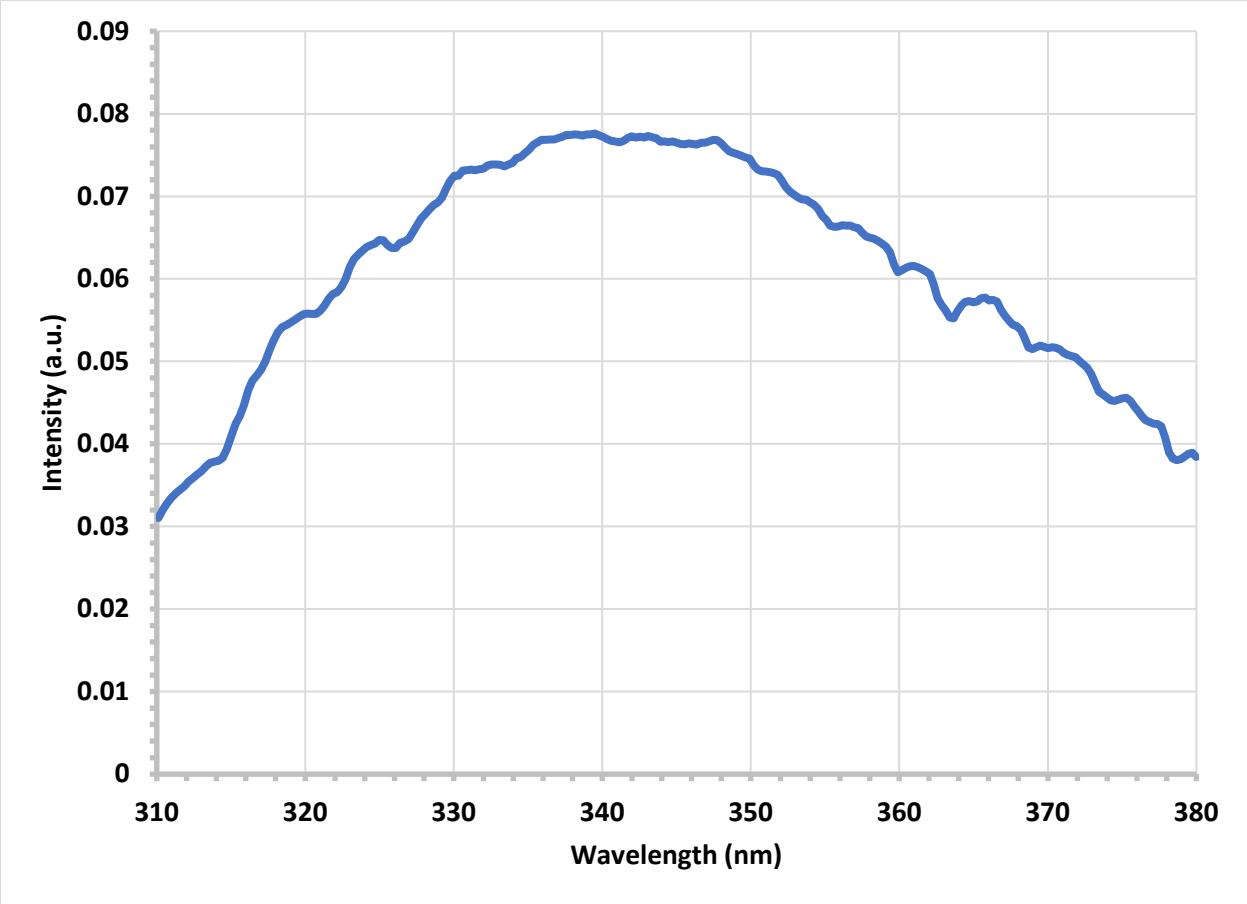

Figure 15: PCA Principal Component 1 plot for UV irradiation experiment on *E. coli* bacteria ($\approx 10^8$ cells/mL).

For this experiment, *E. coli* bacteria ($\approx 10^8$ cells/mL) were irradiated for 0 minutes, 5 minutes, and 20 minutes by means of the onboard disinfection unit. At each time step, 10 normal fluorescence spectra ($\lambda_{EX} \approx 285$ nm) were acquired with the disinfection unit as the excitation source. The fluorescence data in the range of 310-380 nm, which was found to provide the best clustering, was then subjected to PCA by means of the processing GUI. Essentially, the PCA score plot shown in Figure 14 treats each fluorescence spectrum as a single object, thereby reducing the dimensionality of the original dataset; the objects are separated along the principal component 1 (PC1) and principal component 2 (PC2) axes, with the majority of variation occurring along the PC1 axis, as expected. This plot serves as a visual means of separating and identifying bacteria as a function of the UV dosage, which we expect to be correlated with the fraction of bacteria inactivated. Therefore, this procedure allows for the identification of live and dead bacteria samples. It is worthy to mention that the clustering in this score plot may be improved by either (a) acquiring more spectra for processing or (b) performing median-filtering on the data to further reduce noise.

The PC1 component plot shown in Figure 15 demonstrates that while the score plot reduces the dimensionality of the dataset, the principal components, which account for the variation between PCA objects, maintain the same dimensionality as the dataset. Such component plots provide critical information as to the exact regions of difference, or variation, between

each PCA object. For our experiments, it was found that practically all variation was captured in PC1 alone. Therefore, the PC2 component plot is excluded from this subsystem report.

2.3.3. Excitation Monochromator Subsystem Communication

The validation of the excitation monochromator subsystem communication is already provided through the previous EEM and synchronous fluorescence data shown in Figure 11, Figure 12, and Figure 13. The acquisition of this data involved communication with the excitation monochromator, namely the calibration and rotation of the excitation grating across a range of excitation wavelengths, and therefore validates this subsystem requirement. Further validation on the accuracy of the experimental data is provided in the excitation monochromator and emission monochromator subsystem reports.

Additionally, it is worthy to mention that at any point when a communication failure with the excitation monochromator subsystem was detected, the program would write an error message and cease execution.

2.3.4. Emission Monochromator Subsystem Communication

The validation of the emission monochromator subsystem communication is already provided through the previous normal fluorescence, EEM, and synchronous fluorescence data shown in Figure 10, Figure 11, Figure 12, and Figure 13. The acquisition of this data involved communication with the emission monochromator, namely the configuration of acquisition parameters and subsequent receival of spectral data, and therefore validates this subsystem requirement.

Additionally, it is worthy to mention that the query commands noted in Table 4 were utilized in the MATLAB code as a means of ensuring acquisition parameters were properly communicated to the emission monochromator subsystem. At any point when a communication failure was detected, the program would write an error message and cease execution.

2.4. Subsystem Conclusion

In conclusion, this subsystem satisfies all required functionalities. Namely, it is capable of receiving inputs from the user, communicating with both the excitation monochromator and emission monochromator subsystems, processing data, and outputting data, including both acquired spectra and PCA results. Communication with both the excitation monochromator and emission monochromator subsystems was validated, along with the functionalities of the acquisition and processing GUIs. For next semester, the acquisition and processing GUIs will be combined into a single GUI, and perhaps deployable application, which integrates the acquisition and processing capabilities.

3. Disinfection Unit Subsystem Report

3.1. Subsystem Introduction

The disinfection unit subsystem may serve as both a (1) disinfection source for inactivating bacteria *in-situ* and as an (2) excitation source for normal fluorescence measurements. This provides a very efficient means of inactivating bacteria, observing the resulting changes in the normal fluorescence spectra, and confirming the disinfection was successful. To accomplish these functionalities, a high-power, miniature UV LED is used, along with excitation and collection optics for maximizing the fluorescence intensity. These components are housed in a lightweight, portable enclosure.

3.2. Subsystem Details

3.2.1. Components

A picture of the current embodiment for the disinfection unit subsystem, along with its major components, is shown in Figure 16 below.

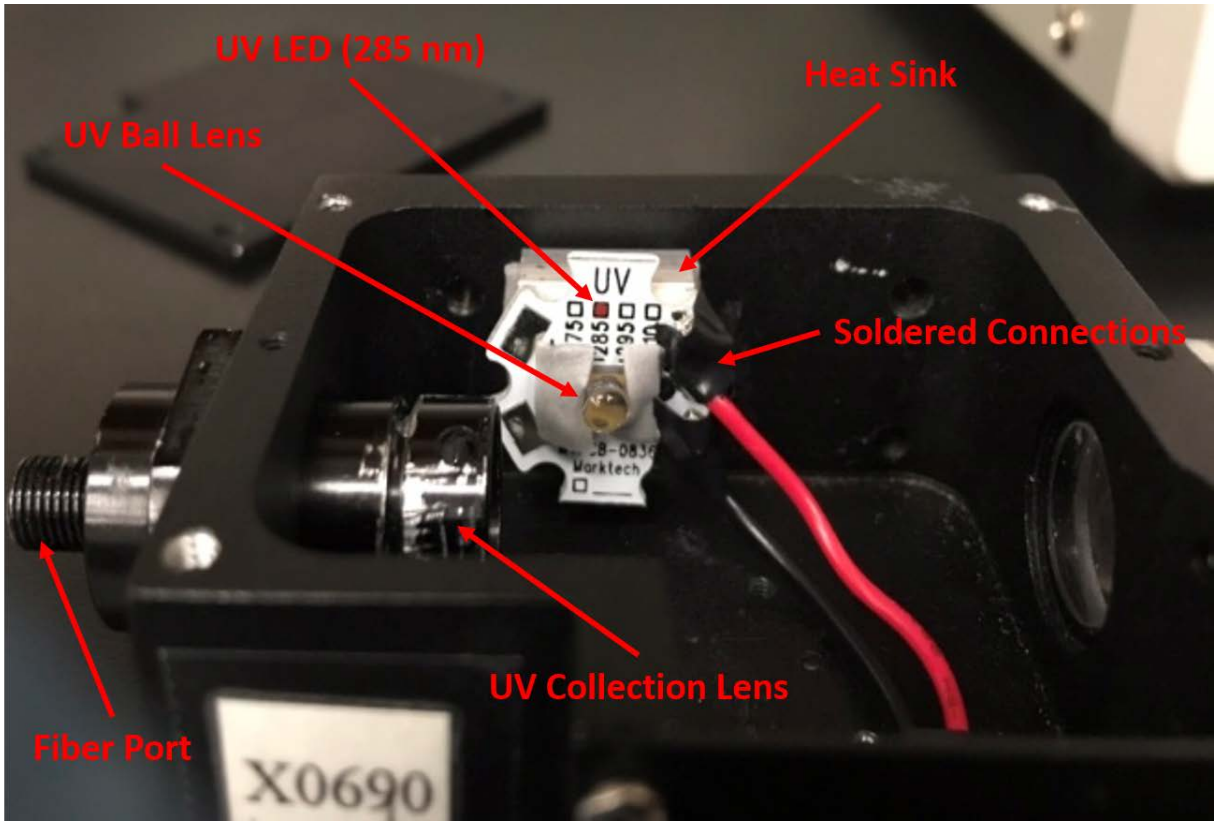

Figure 16: Disinfection unit subsystem and its major components.

The disinfection unit currently consists of a high-power, miniature UV LED (MTSM285UV-F1120S) mounted on a heat sink and coupled with a UV ball lens. The UV LED is attached to the heat sink by means of a thermal adhesive to promote efficient heat dissipation, which is critical in ensuring stable LED operation. A UV ball lens is utilized as a means of collecting

and focusing the output of the LED, which is otherwise diverging. This increases the excitation intensity and subsequent fluorescence from the bacterial sample. Since the fluorescence of the sample is diverging as well, a UV collection lens is utilized for collecting and focusing the fluorescence onto an optical fiber positioned at the fiber port. This optical fiber is coupled to the input port of the emission monochromator. The enclosure, fiber port, and collection lens holder are all off-the-shelf components from B&W Tek.

3.2.2. UV LED

Selection of the UV LED is a particularly critical design choice in ensuring that the functionalities of disinfection and excitation are both satisfied by a single LED. To that effect, the germicidal effectiveness curve, indicating the efficacy of various UVB and UVC wavelengths on inactivating bacteria, is provided in Figure 17 below.

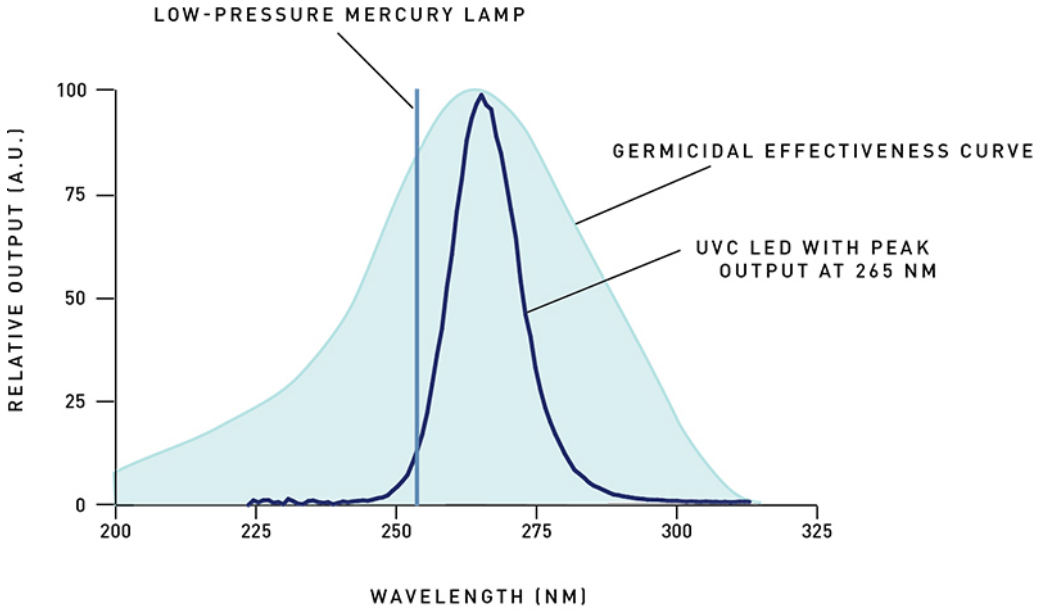

Figure 17: Germicidal effectiveness curve [4].

The plot in Figure 17 suggests that to achieve maximum germicidal effectiveness, a UVC wavelength of approximately 265 nm should be used. The primary reason for this is that this wavelength corresponds to the absorption band of DNA. The absorption of UV light by DNA results in damage to its structure [4], which consequently inhibits bacterial replication and is the mechanism by which bacteria are inactivated. The fluorescence of bacteria, however, is primarily due to tryptophan and tyrosine residues, rather than DNA, which possess absorption bands at higher wavelengths in the UVB and UVC region (≈ 270-290 nm) [5]. Tryptophan, in particular, is known to be the most intensely fluorescing component of bacteria with an absorption band maximum at (≈ 280 nm) [5]. Therefore, a central wavelength of 285 nm was selected for the UV LED to provide both the excitation and disinfection functionalities. As shown in Figure 17, a UV wavelength of 285 nm still provides a rather high germicidal effectiveness.

To that effect, the nominal output spectrum of the selected UV LED is shown in Figure 18 below, along with its nominal characteristics in Table 5.

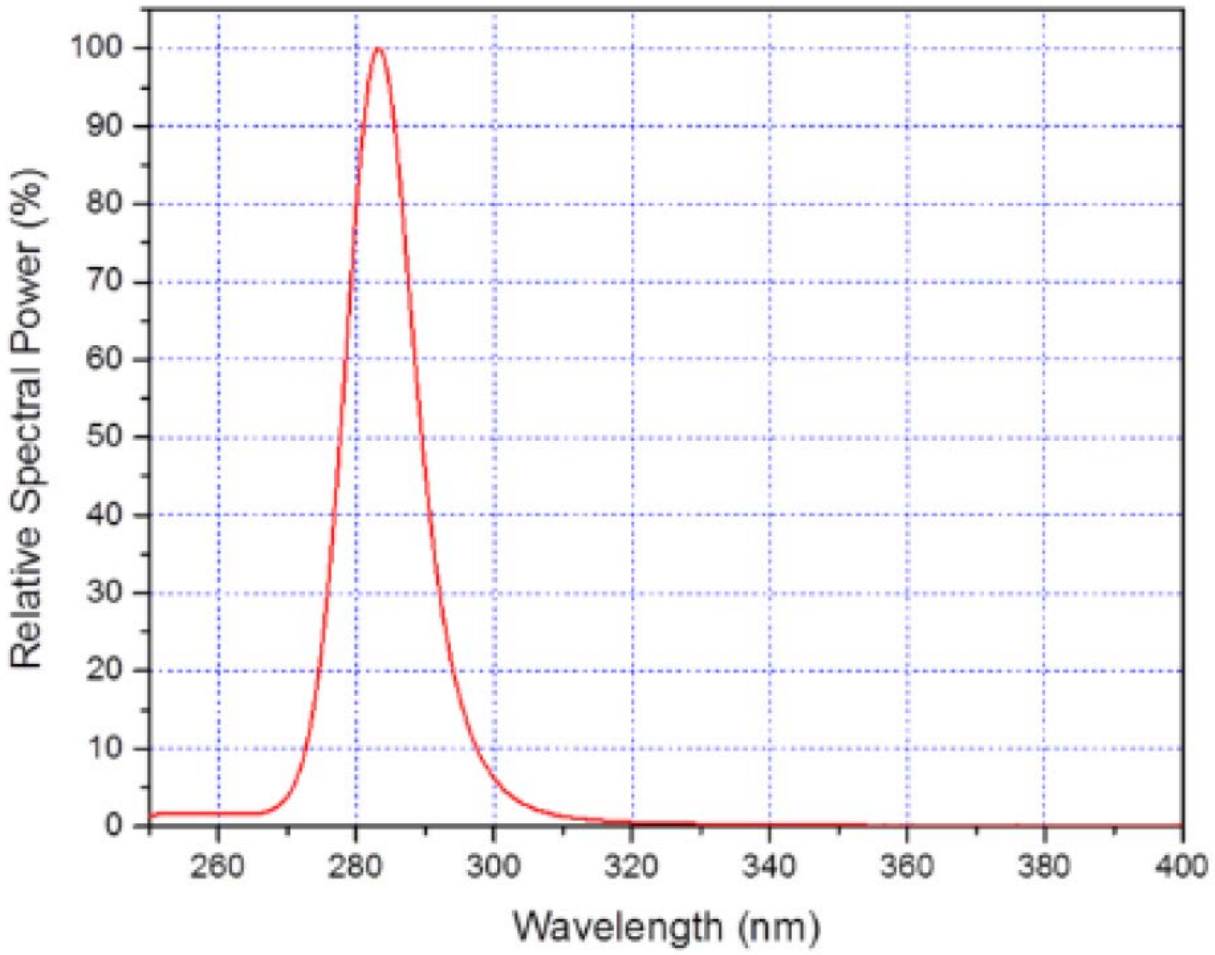

Figure 18: Output spectrum of selected UV LED for disinfection unit (MTSM285UV-F1120S) [6].

Specification	Condition	Minimum	Maximum
Peak Wavelength (nm)	$I_F = 20$ mA	280	290
Power Output (mW)	$I_F = 20$ mA	1.0	2.0
Forward Voltage (V)	$I_F = 20$ mA	5.0	7.0
FWHM (nm)	$I_F = 20$ mA	10.0	15.0

Table 5: Nominal electrical and optical characteristics of selected UV LED [6].

The specifications for the peak wavelength and FWHM of the UV LED indicate that it is a suitable component for functioning as both a disinfection and excitation source, as its most intense emission wavelengths correspond to the absorption bands of tryptophan and tyrosine, along with possessing high germicidal effectiveness. Slight deviations in the exact peak emission wavelength are not expected to drastically affect the excitation and disinfection functionalities.

3.2.3. Operation

The operation of the disinfection unit subsystem is shown in Figure 19 below.

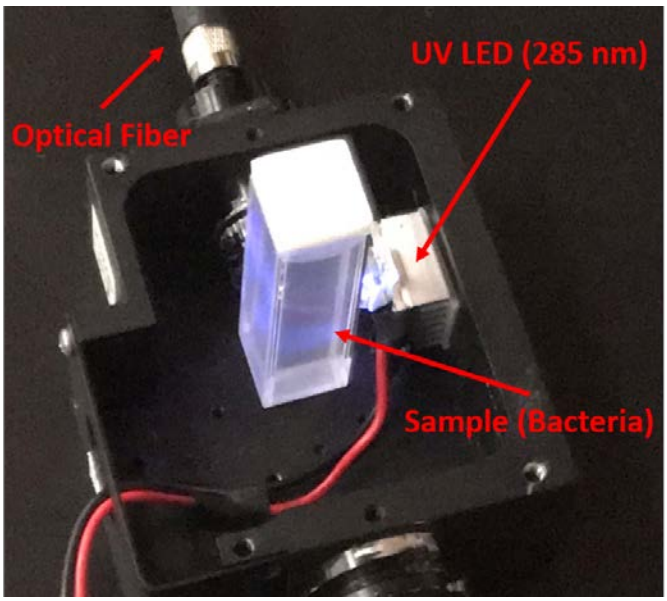

Figure 19: Operation of disinfection unit.

The UV LED was biased to operate at a forward current of approximately 25 mA, which is within its absolute maximum ratings. Power was supplied by a benchtop, regulated DC power supply. The bacterial sample is located at approximately the center of both the UV collection lens and UV LED. This maximizes the fluorescence coupled to the optical fiber and transmitted to the emission monochromator subsystem. A cover for the enclosure will be designed and fabricated next semester to minimize background (stray) light interference. Figure 20 below shows the effect of attaching the UV ball lens to the UV LED when it is turned on.

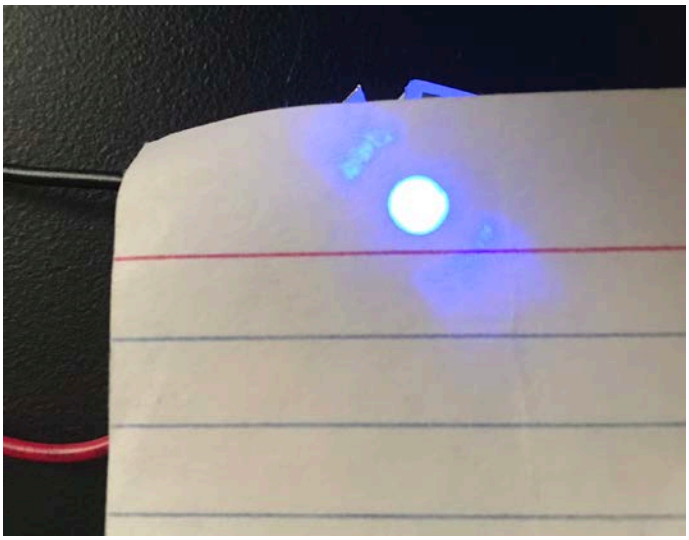

Figure 20: Effect of attaching a UV ball lens to the UV LED.

With the UV ball lens, the output light is more focused and results in a higher excitation intensity, which increases both the sample fluorescence and disinfection rate. When coupled to the emission monochromator subsystem, the disinfection unit may simultaneously inactivate bacteria and serve as an excitation source for normal fluorescence measurements. This serves as an efficient means of monitoring changes in the fluorescence of a bacterial sample, indicative of the fraction of bacteria inactivated, as a function of the UV irradiation time.

3.3. Subsystem Validation

3.3.1. Excitation Source Functionality

The functionality of the disinfection unit as an excitation source was validated by recording the normal fluorescence of tyrosine (≈ 1 mg/mL), tryptophan (≈ 1 mg/mL), and *E. coli* bacteria (≈ 10^8 cells/mL) with the emission monochromator subsystem.

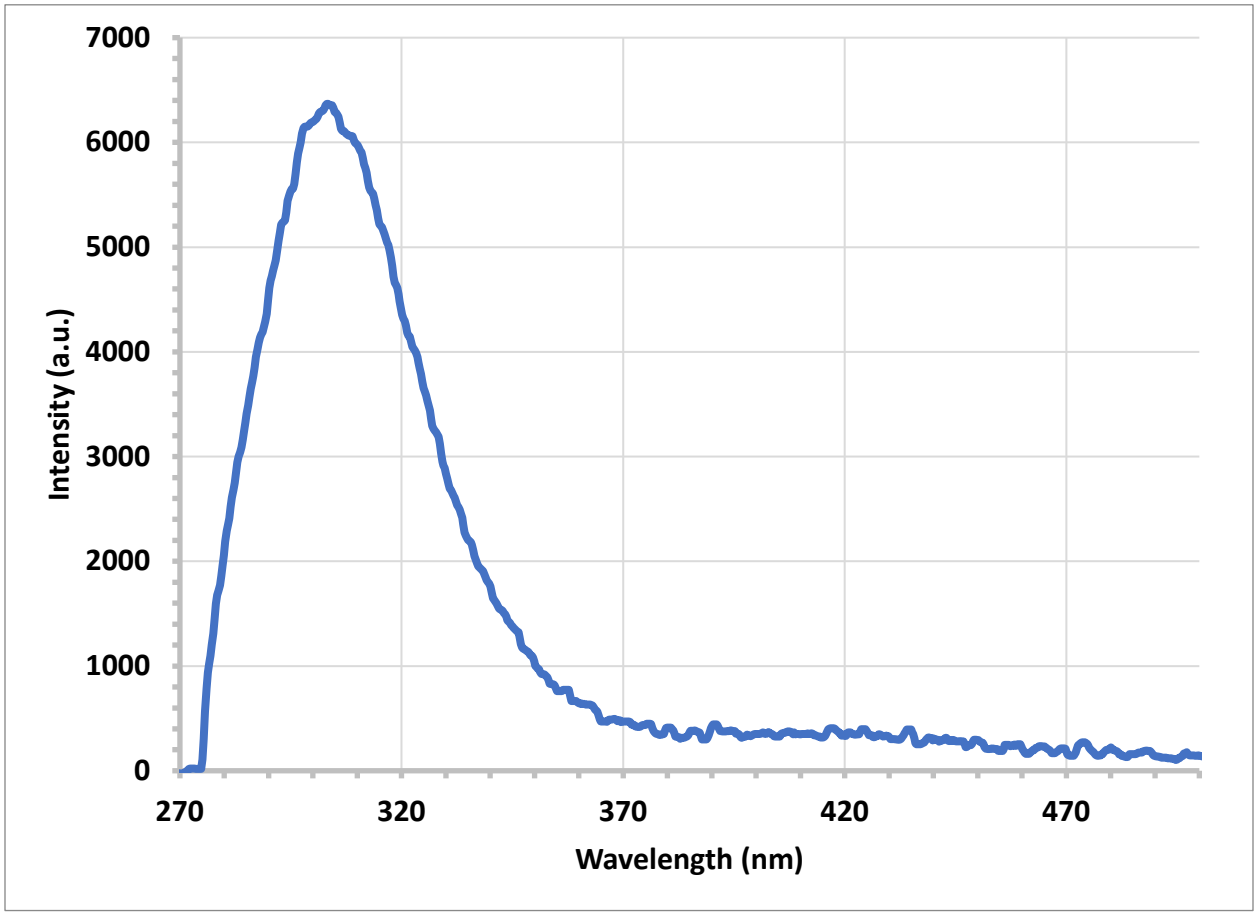

Figure 21: Normal fluorescence (λ_{EX} ≈ 285 nm) spectrum of tyrosine (≈ 1 mg/mL) acquired with the disinfection unit as the excitation source.

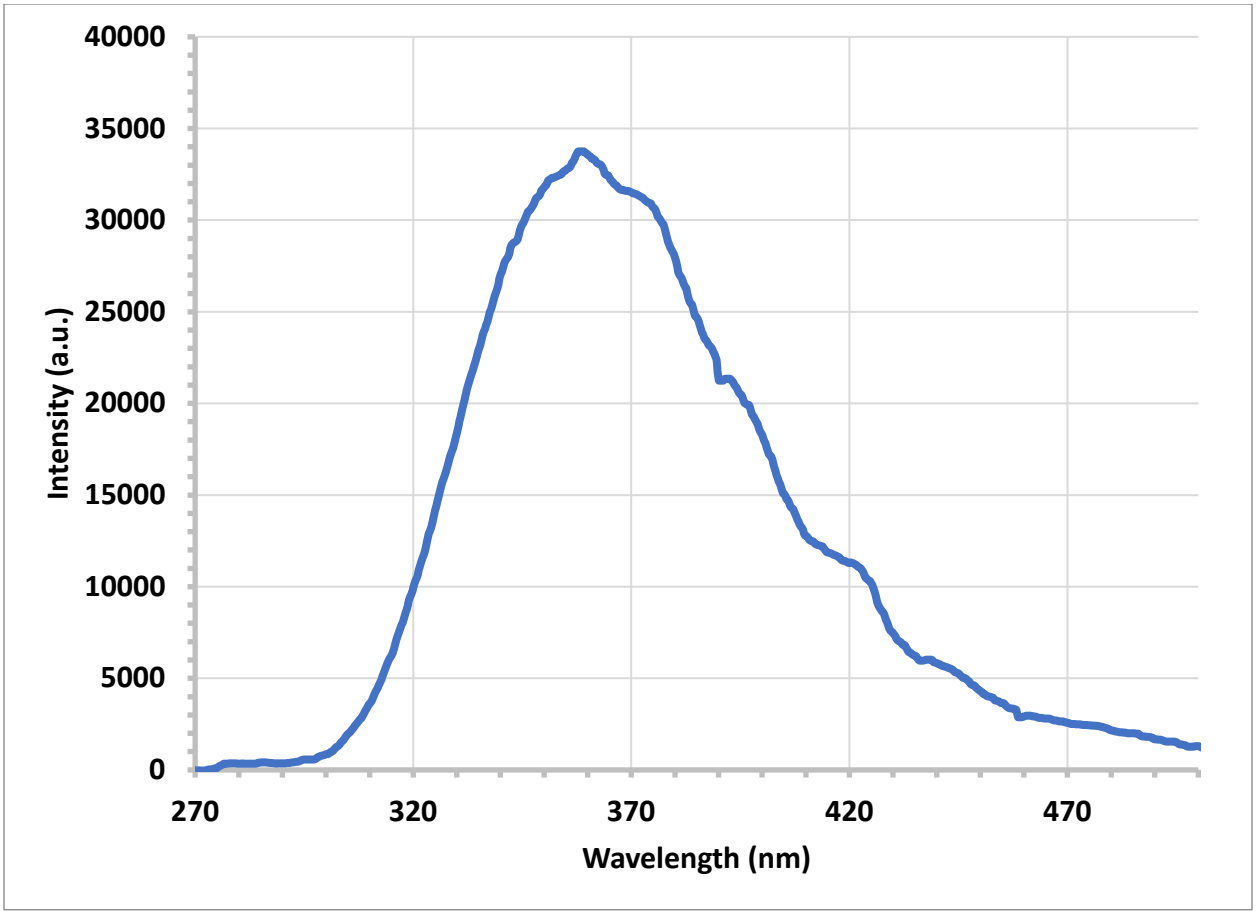

Figure 22: Normal fluorescence ($\lambda_{EX} \approx 285$ nm) spectrum of tryptophan (≈ 1 mg/mL) acquired with the disinfection unit as the excitation source.

In comparing Figure 21 and Figure 22, it is of relevance to observe the differences in the normal fluorescence spectra of tyrosine and tryptophan at $\lambda_{EX} \approx 285$ nm, namely the region of maximum fluorescence and the peak fluorescence intensity itself. A more comprehensive validation of these normal fluorescence measurements is provided in the excitation monochromator and emission monochromator subsystem reports.

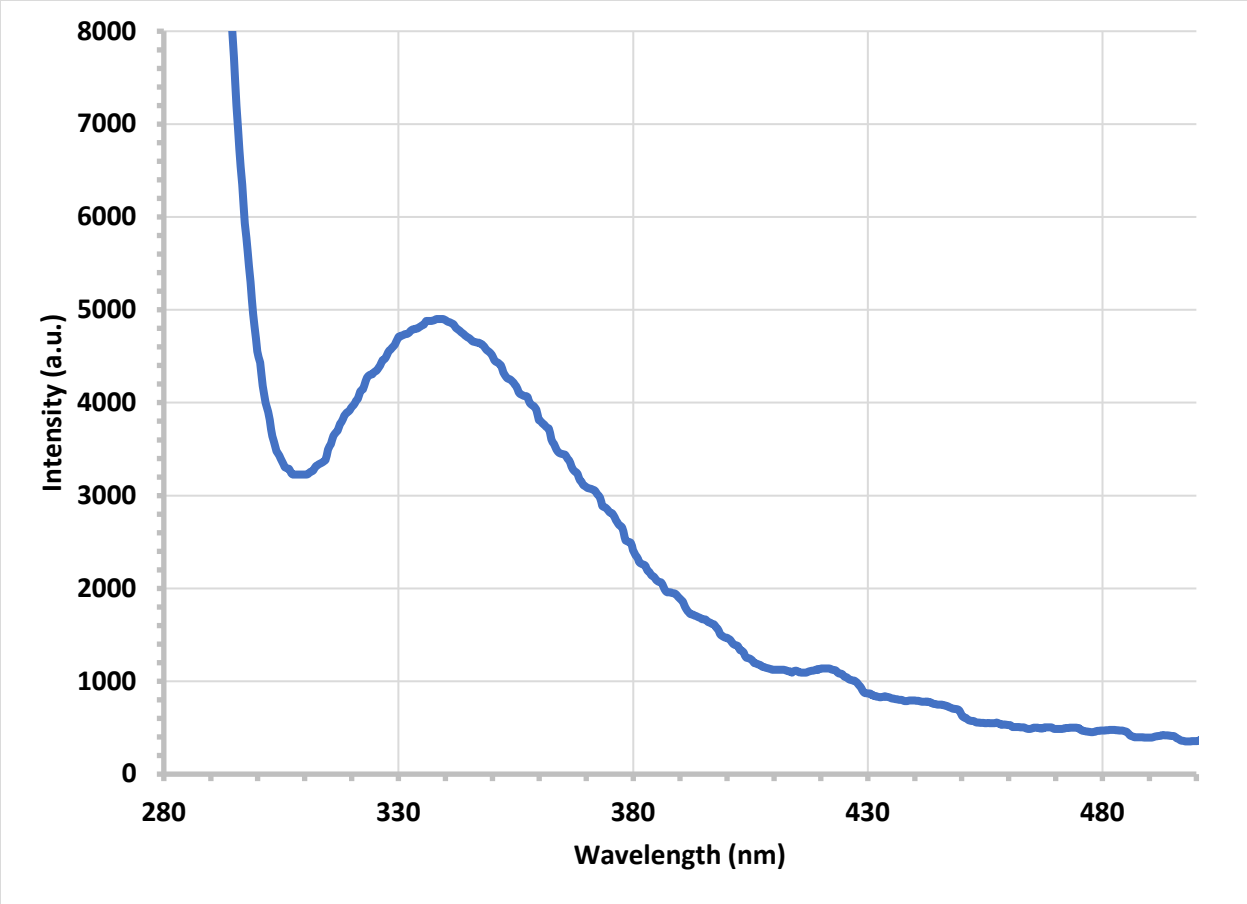

Figure 23: Normal fluorescence ($\lambda_{EX} \approx 285$ nm) spectrum of *E. coli* bacteria ($\approx 10^8$ cells/mL) acquired with the disinfection unit as the excitation source.

The initially high intensity is due to Rayleigh (elastic) scattering of the excitation beam and may be used as a means of estimating the peak emission wavelength of the LED. The fluorescence band of *E. coli* is clearly observed with a maximum at approximately 340 nm. This fluorescence is due, primarily, to tryptophan and tyrosine residues within the bacterial cells. The detection of this band is therefore a validation of the excitation functionality of the disinfection unit. A more comprehensive validation of this normal fluorescence measurement is provided in the excitation monochromator and emission monochromator subsystem reports.

3.3.2. Disinfection Source Functionality

The functionality of the disinfection unit as an excitation source was validated by recording the normal fluorescence of *E. coli* bacteria ($\approx 10^8$ cells/mL) as a function of varying irradiation, or disinfection, times. The disinfection unit was therefore used as both an excitation and disinfection source for this experiment.

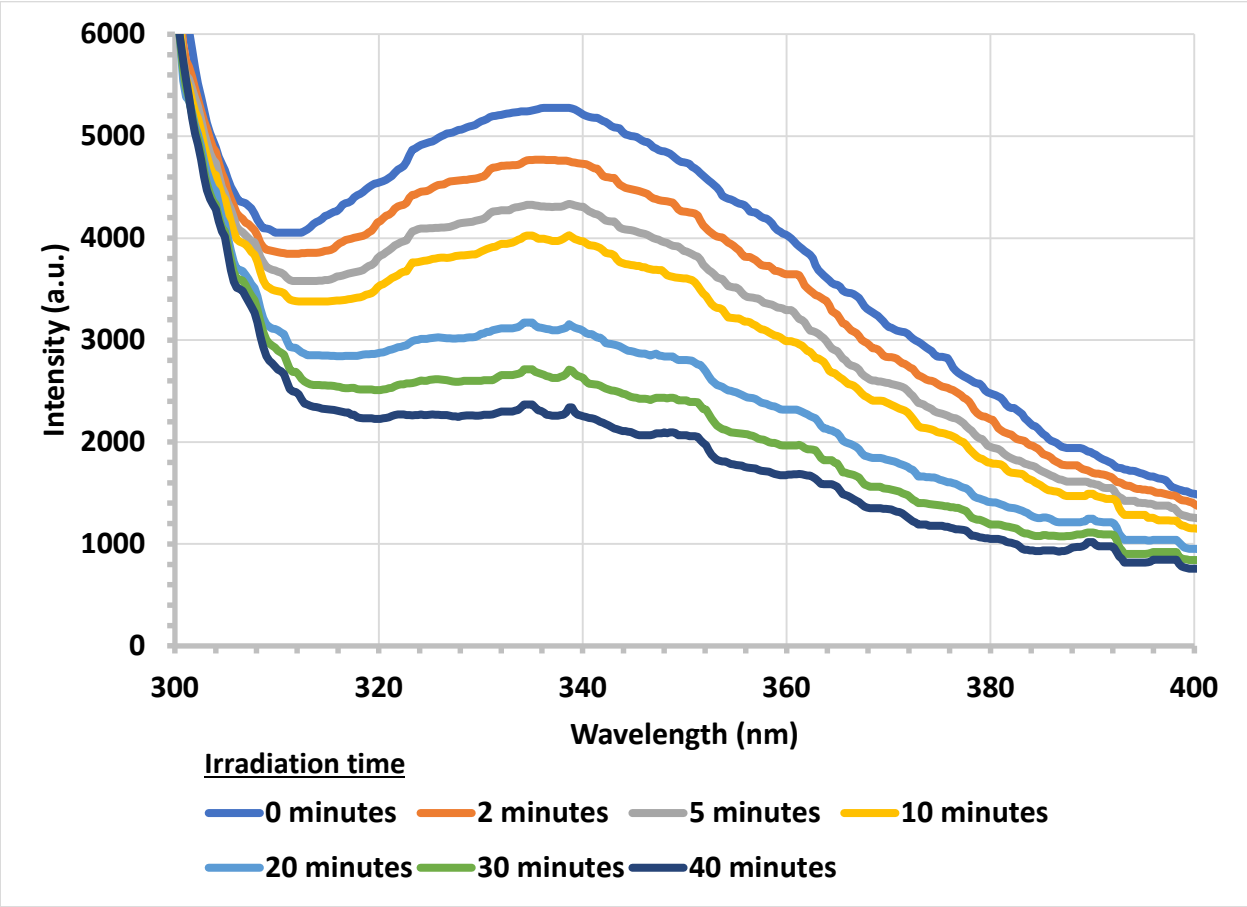

Figure 24: Normal fluorescence ($\lambda_{EX} \approx 285$ nm) spectra of *E. coli* bacteria ($\approx 10^8$ cells/mL) as a function of disinfection time.

In this experiment, the irradiation time varied from 0-40 minutes in varying time steps. Clearly, the fluorescence spectra of *E. coli* decrease continuously as a function of the irradiation time. To further investigate this decrease, the fluorescence band maximum, or peak intensity, was plotted as a function of irradiation time.

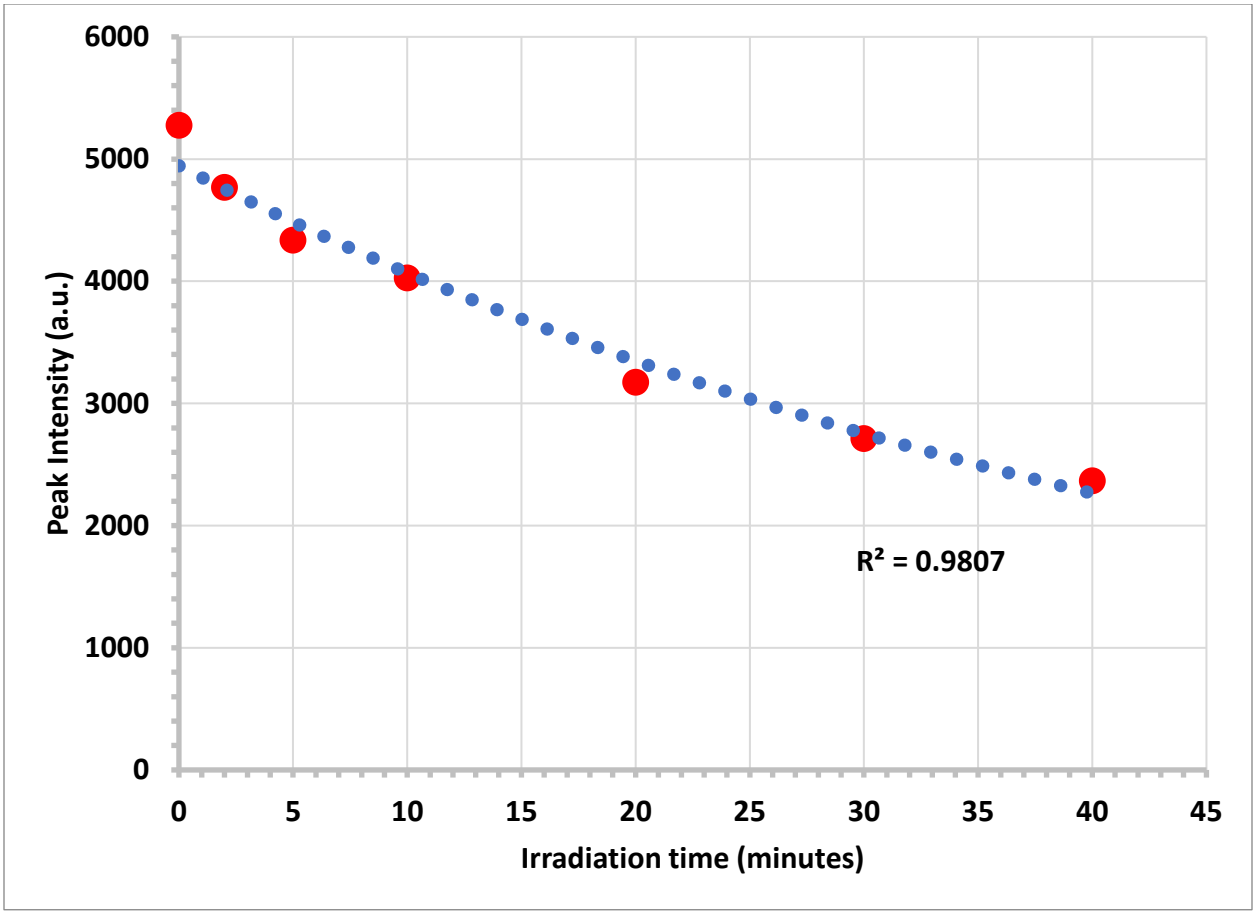

Figure 25: Peak fluorescence intensity as a function of irradiation time.

The experimental data in Figure 25 is plotted with an exponential fit. This suggests that the peak fluorescence intensity decays exponentially as a function of the irradiation time. The nature of this fluorescence decay will be investigated in more detail next semester. Nonetheless, it is well known that both tryptophan and tyrosine degrade in response to UV exposure, which results in a decrease in fluorescence [7]. This degradation, in turn, is correlated with damage to DNA and the subsequent inactivation of bacteria. We may therefore interpret the decrease in fluorescence as a validation of the disinfection capability of this subsystem. Furthermore, the inherent germicidal effectiveness of the UV LED wavelength is a rather strong confirmation of this functionality.

3.4. Subsystem Conclusion

In conclusion, this subsystem satisfies all required functionalities. Namely, it is capable of serving as both an excitation source for normal fluorescence measurements, as well as a disinfection source for irradiating and inactivating bacterial samples. The design and fabrication of a cover for the disinfection unit will be completed next semester. In addition, the exact nature of the inactivation process will be further investigated and quantified next semester.

4. Excitation Monochromator Subsystem Report

4.1. Subsystem Introduction

The excitation monochromator subsystem serves as a scanning excitation source for performing EEM acquisition and acquiring synchronous fluorescence spectra. It is composed of a (1) high-power, miniature UV LED as an excitation source, (2) a scanning monochromator coupled with a stepper motor for selecting a particular excitation wavelength from the LED spectrum, and (3) a stepper motor controller and driver for rotating the excitation grating. Commands are issued to this subsystem through a serial communication link between the computer and controller. These components are housed in a lightweight, portable enclosure.

4.2. Subsystem Details

4.2.1. Components

A picture of the current embodiment for the excitation monochromator subsystem, along with its major components, is shown in Figure 26 below.

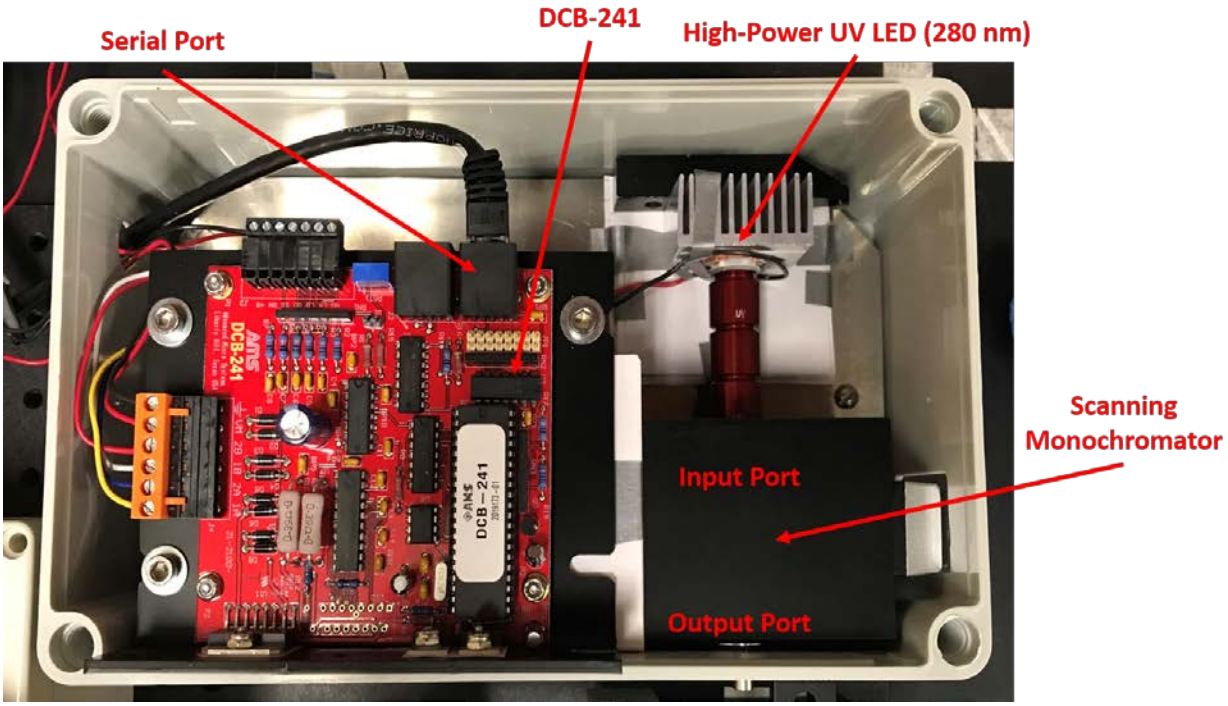

Figure 26: Excitation monochromator subsystem and its major components.

The excitation monochromator currently consists of a high-power miniature UV LED (RVXP4-280-SM-077132) mounted on a heat sink and coupled with a set of three UV lenses. Similar to the disinfection unit, the UV LED is attached to the heat sink by means of a thermal adhesive to promote efficient heat dissipation, which is critical in ensuring stable LED operation. The three UV lenses are necessary for collecting and reducing the divergence of the LED output and ensuring good coupling is achieved with the scanning monochromator,

which principally determines the excitation intensity at the sample location and consequent fluorescence intensity.

The scanning monochromator is an off-the-shelf component from Dynasil. The monochromator consists of an optical bench housing two folding mirrors, a single curved mirror, and a reflective diffraction grating. The function of this component is to disperse the broadband UV light from the LED and focus a particular wavelength of the dispersed light on the exit slit of the monochromator. The particular wavelength of the dispersed light focused on the exit slit will be dependent on the angular positioning of the excitation grating and controlled by an onboard stepper motor. To that effect, EEM acquisition can occur by rotating the excitation grating and therefore scanning over a range of excitation wavelengths.

The integrated stepper motor controller and driver is the DCB-241, which was previously described in detail in the control and display unit subsystem report. The controller is wired to the stepper motor within the monochromator through an external DB-15 connector. Communication with the controller is achieved through the onboard serial port.

A mounting plate for this subsystem was designed and fabricated through the Physics Machine Shop at Texas A&M University with the assistance of Mr. Garrick Garza. A cheap, compact electronics project box was utilized as the enclosure. A picture of the overall design is shown in Figure 27 below.

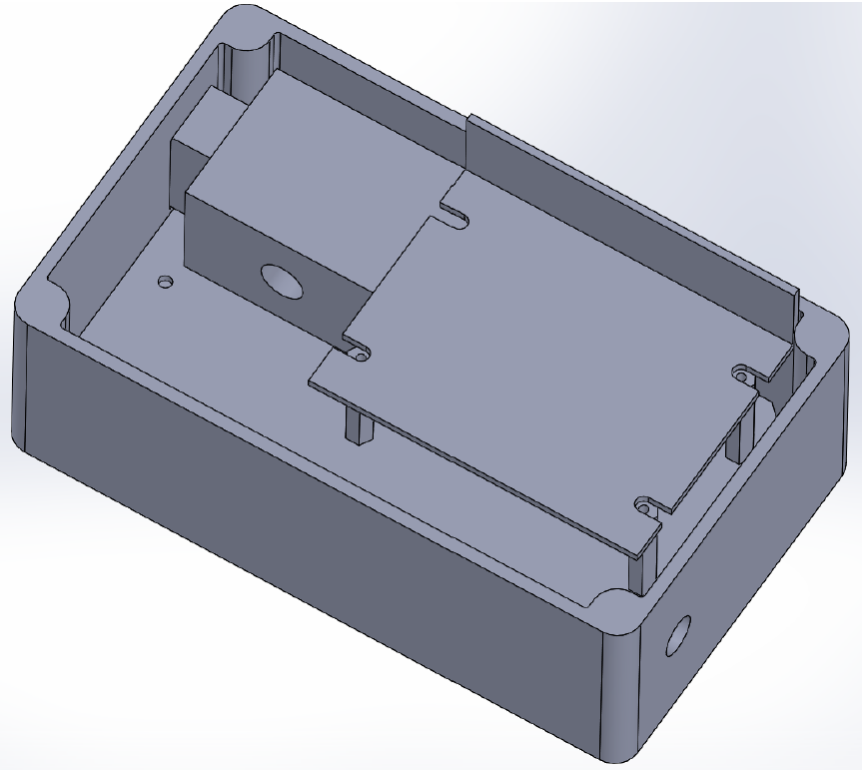

Figure 27: Design for the excitation monochromator subsystem, including the enclosure and mounting plate.

4.2.2. UV LED

Selection of the UV LED wavelength was guided, mainly, by the same considerations noted in the disinfection unit subsystem report. Owing to the fact that the LED output passes through a monochromator in this subsystem, however, an LED with a significantly higher output power was selected. This is necessary to account for both (a) coupling losses at the input of the monochromator and (b) diffraction losses within the monochromator itself, which will significantly reduce the excitation intensity at the sample location.

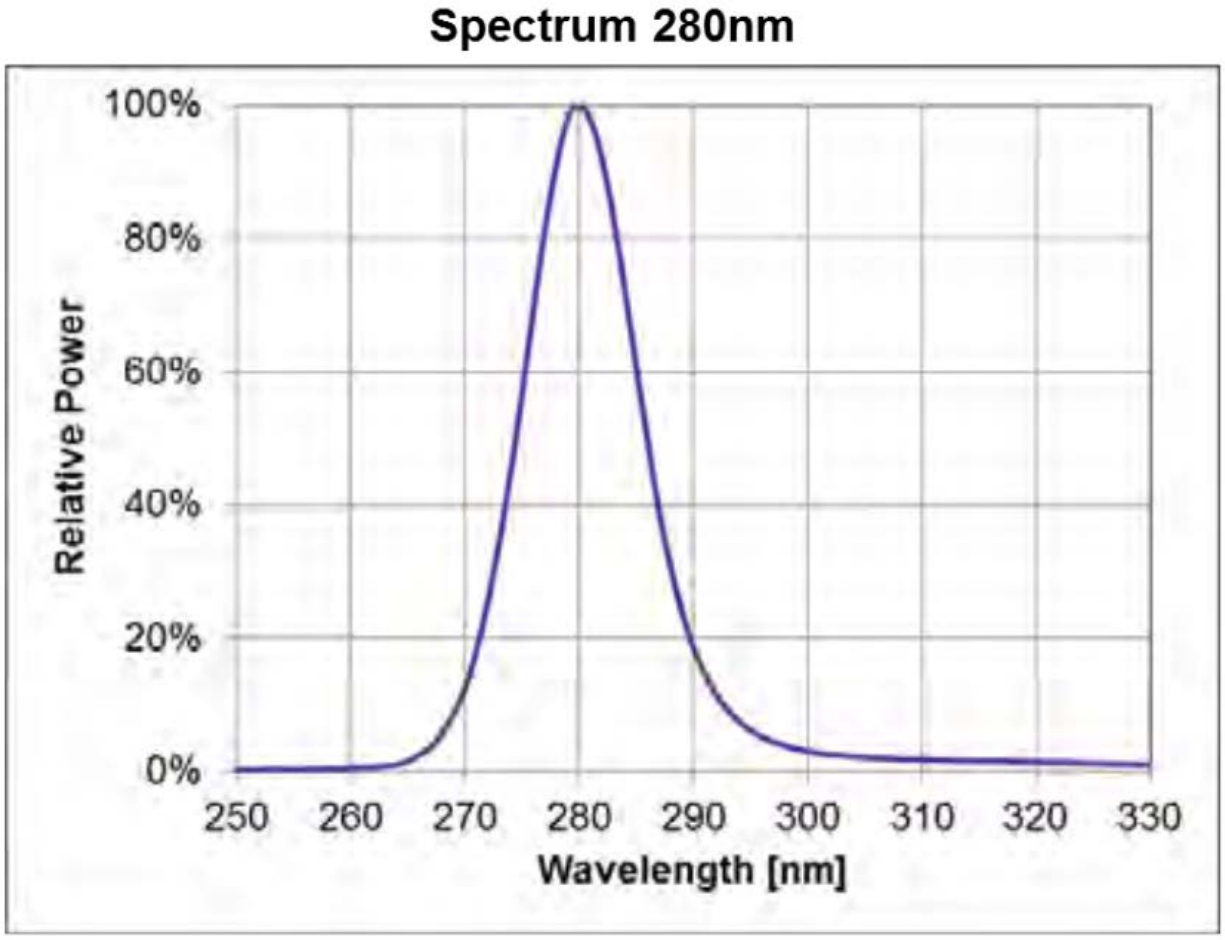

Figure 28: Output spectrum of selected UV LED for excitation monochromator (RVXP4-280-SM-077132) [8].

Specification	Condition	Minimum	Typical	Maximum
Peak Wavelength (nm)	$I_F = 200$ mA	275	280	285
Power Output (mW)	$I_F = 200$ mA	30	50	70
Forward Voltage (V)	$I_F = 200$ mA	20	26	32
FWHM (nm)	$I_F = 200$ mA	Not given.	15	Not given.

Table 6: Nominal electrical and optical characteristics of selected UV LED [8].

Clearly, the selected UV LED for the excitation monochromator has a significantly higher optical power than that used for the disinfection unit. This output power is among the highest, if not the highest, radiant output available for current UV LED technology.

4.2.3. Scanning Monochromator

The scanning monochromator selected for this subsystem is the Scanning Digital Mini-Chrom Monochromator (SDMC1-02) sold by Dynasil. The optical layout for this component is provided in Figure 29 below.

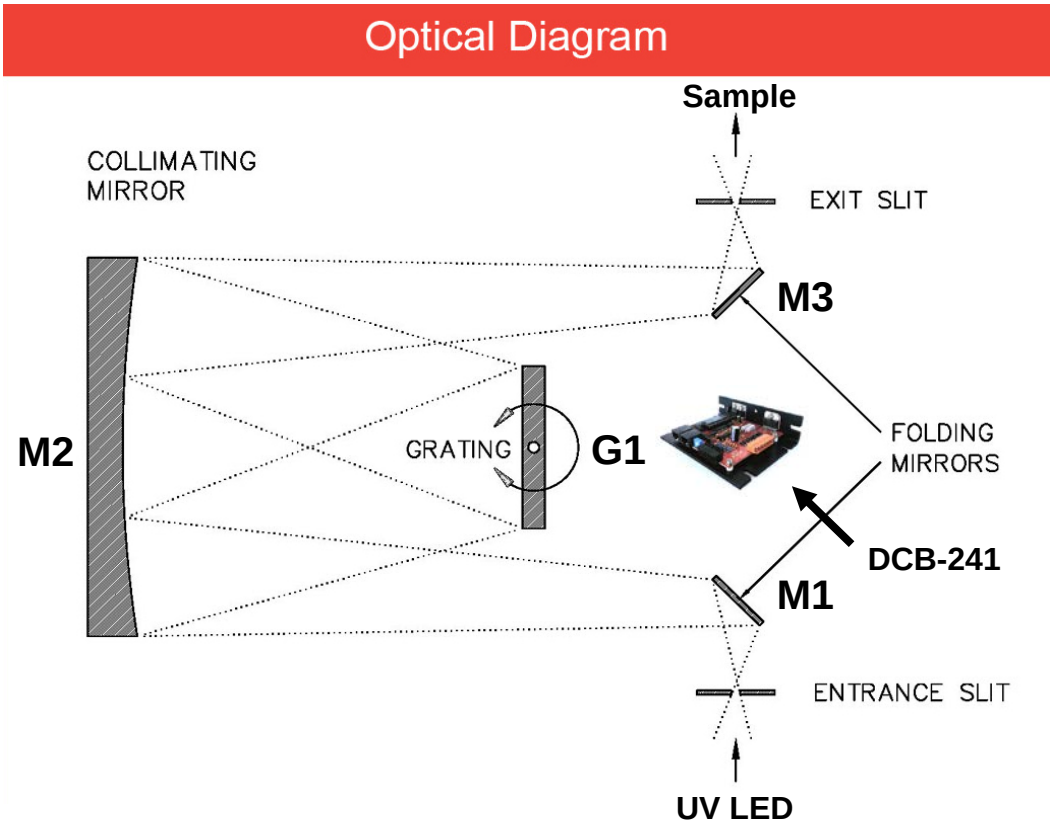

Figure 29: Schematic of the scanning monochromator in the excitation monochromator subsystem [9].

The monochromator optical bench houses a Fastie-Ebert configuration, consisting of two folding mirrors M1 and M3, a single curved mirror M2, and a reflective diffraction grating G1. The high-power, miniature UV LED is coupled to the bench at the entrance slit, whereupon the input, broadband UV light is reflected by M1 to M2. M2 then collimates and directs the light to the reflective grating G1, which diffracts and disperses the light into its component wavelengths. The dispersed light is reflected from G1 to M2 again, which focuses the light to the exit slit by means of M3. The particular wavelength of the dispersed light focused on the exit slit is dependent on the angular positioning of the excitation grating G1. To that effect,

the DCB-241 rotates a stepper motor within the monochromator connected to the excitation grating. This allows for rotation to a desired output wavelength or, alternatively, through a range of excitation wavelengths, as desired in an EEM acquisition. An optical fiber may optionally be connected at the exit slit to transmit the excitation wavelength to the sample; alternatively, to maximize the excitation intensity, the sample may be directly situated at the exit slit itself. It is worthy to mention that all components in the optical bench are optimized for performance in the UV spectral region, particularly the grating.

4.2.4. DCB-241

The DCB-241 was described in detail in the control and display unit subsystem report. The commands provided in Table 2 of that report were utilized to set the initial and final slew velocity of the stepper motor within the scanning monochromator, rotate the stepper motor and excitation grating, and thereby perform EEM acquisitions when coupled with the emission monochromator subsystem. To supplement that information, some additional electrical specifications of the component are provided below.

Specification	Value
Input Voltage (V)	+24 to 40 V DC
Motor Step Resolution	Half Step

Table 7: Electrical specifications of the DCB-241.

4.2.5. Operation

The UV LED was biased to operate at a forward current of approximately 100 mA, which is well within its absolute maximum ratings. This bias point was selected to ensure stable operation but can be changed for future experiments as needed to increase the excitation intensity. Figure 30 shows the high-power UV LED mounted on a heat sink with the thermal adhesive.

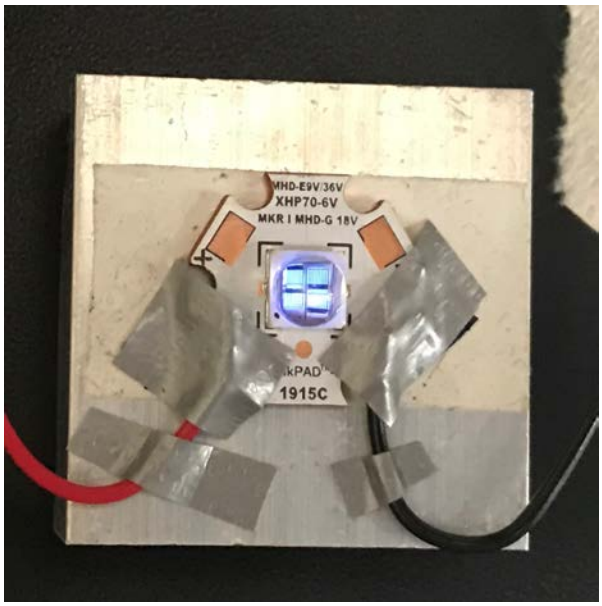

Figure 30: High-power UV LED mounted on heat sink with thermal adhesive.

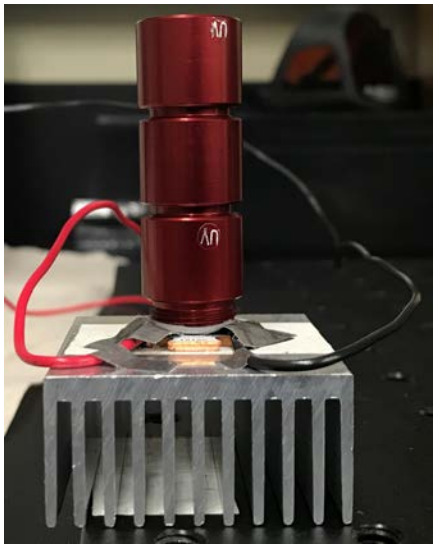

Figure 31: UV coupling lenses mounted on top of high-power UV LED for maximizing excitation intensity.

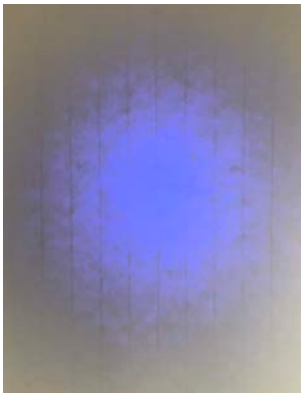

Figure 32: Image of UV LED output without coupling lenses.

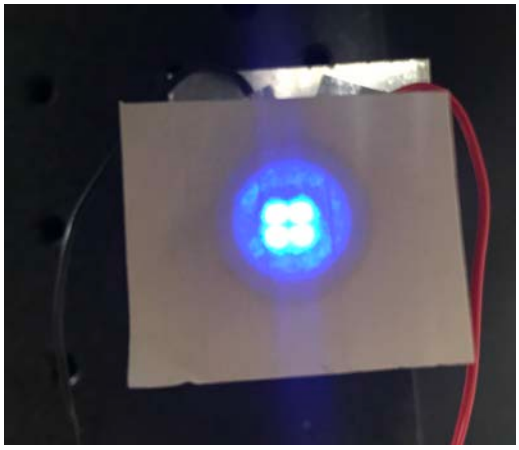

Figure 33: Image of UV LED output with coupling lenses.

As demonstrated in Figure 32 and Figure 33, the UV coupling lenses are critical in capturing a large fraction of the rapidly diverging UV light from the LED; the use of three lenses increases the optical power of the overall setup and results in a sharp image of the emitting surfaces within the LED. Alignment was then performed between the UV LED and input slit of the excitation monochromator to maximize the coupling between the two components.

The DCB-241 was then biased through its onboard potentiometer to output a run current which resulted in stable rotation of the stepper motor within the monochromator. This process involved rotating the onboard potentiometer in small increments and observing the resultant behavior and performance of the stepper motor in rotating the excitation grating. Once a minimum run current was established, it was increased by ≈ 10%. This was done to ensure reliable operation of the stepper motor and minimize heating due to large run currents.

The initial and final slew velocities of the stepper motor were then set to the lowest possible values and increased until the stepper motion was deemed sufficiently smooth. This was determined to occur at initial and final slew velocities of 20 steps/second.

To confirm the linearity of the stepper motor, the time required to traverse a range of steps as low as 160 to as high as 1600 was measured and compared with the theoretical time set by the slew velocities. The results of this test are shown in Figure 34 below.

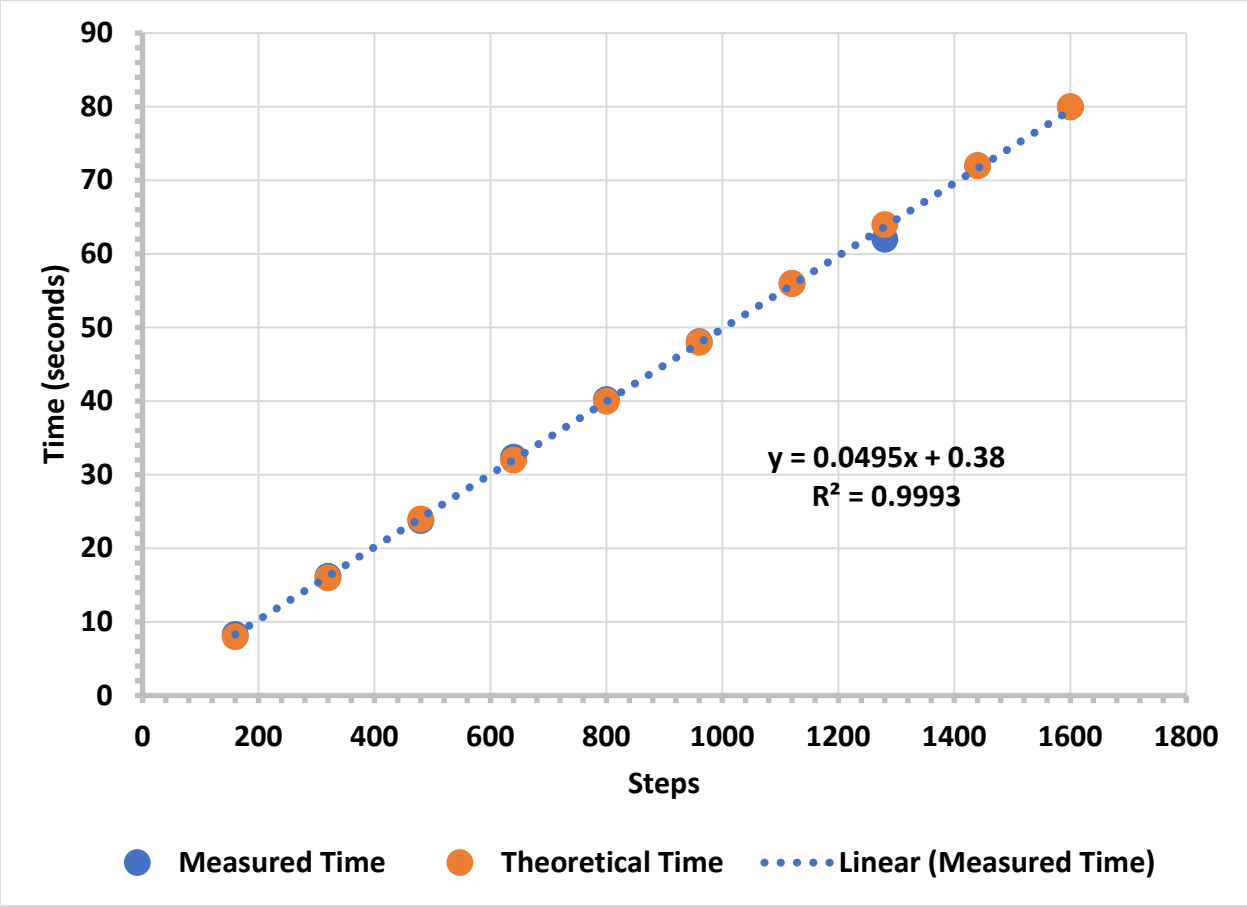

Figure 34: Comparison of measured time and theoretical time for stepper motor rotation.

Figure 34 clearly demonstrates the proper operation of the stepper motor at the biased, run current and initial and final slew velocities. These parameters can be easily adjusted and refined if the stepper motor operation is deemed insufficient at any time. For the experimental data collected this semester, though, such parameters were sufficient in achieving the desired performance of the subsystem.

Power was supplied to both the UV LED and DCB-241 by a benchtop, regulated DC power supply to simplify the validation of the subsystem.

4.3. Subsystem Validation

4.3.1. Experimental Setup for Acquiring EEM

The functionality of the excitation monochromator in recording the EEM of a sample was validated by recording the EEM of tyrosine (≈ 1 mg/mL), tryptophan (≈ 1 mg/mL), a mixture of tyrosine and tryptophan, and *E. coli* bacteria (≈ 10^8 cells/mL). This was accomplished by utilizing the excitation monochromator as a scanning excitation source and detecting the sample fluorescence with the emission monochromator subsystem. A picture of the overall experimental setup that was built for this validation is shown in Figure 35 below.

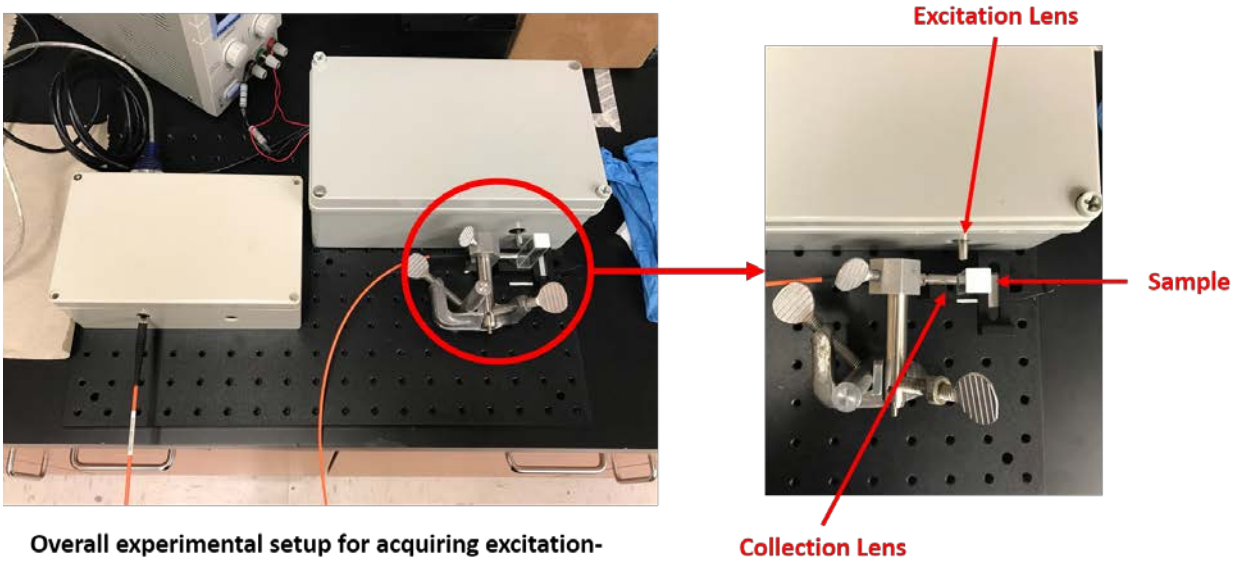

Figure 35: Overall experimental setup for acquiring the excitation-emission matrix (EEM) of a sample.

In brief, the output of the excitation monochromator was focused onto the sample by means of a UV excitation lens. The sample was located at, approximately, the focal point of the excitation lens to maximize the excitation and fluorescence intensity. The sample fluorescence was then captured by a UV collection lens coupled with an optical fiber. The optical fiber then transmitted the sample fluorescence to the input slit of the emission monochromator subsystem. By recording the sample fluorescence over a range of excitation wavelengths, the sample EEM may be acquired.

4.3.2. EEM Acquisition

The EEMs of tyrosine (≈ 1 mg/mL), tryptophan (≈ 1 mg/mL), a mixture of tyrosine and tryptophan, and *E. coli* bacteria (≈ 10^8 cells/mL) are presented below. Synchronous fluorescence spectra are compared with those acquired by a benchtop, commercial spectrometer as validation of the subsystem's operation.

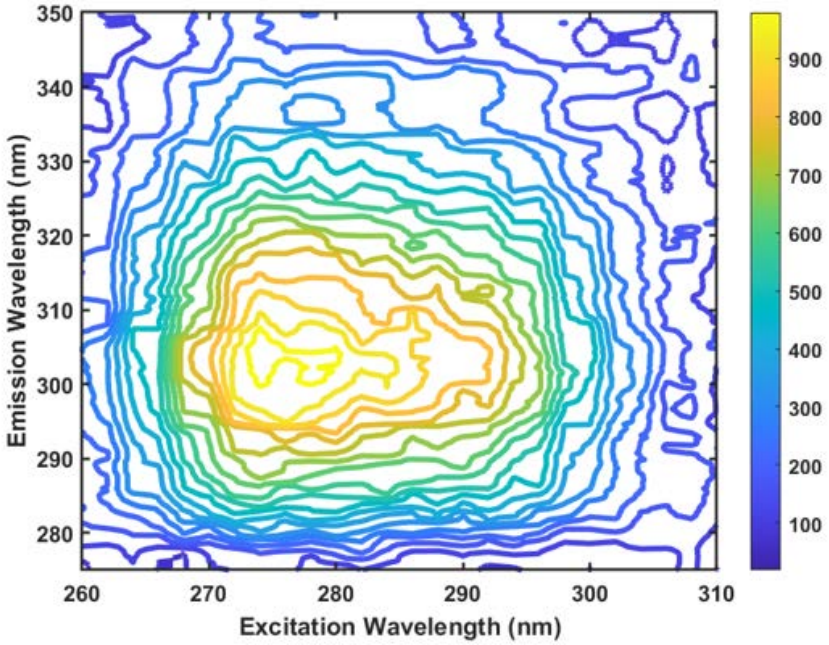

Figure 36: 2D contour plot of EEM for tyrosine (≈ 1 mg/mL) acquired over an excitation range of 260 to 310 nm in 2 nm steps.

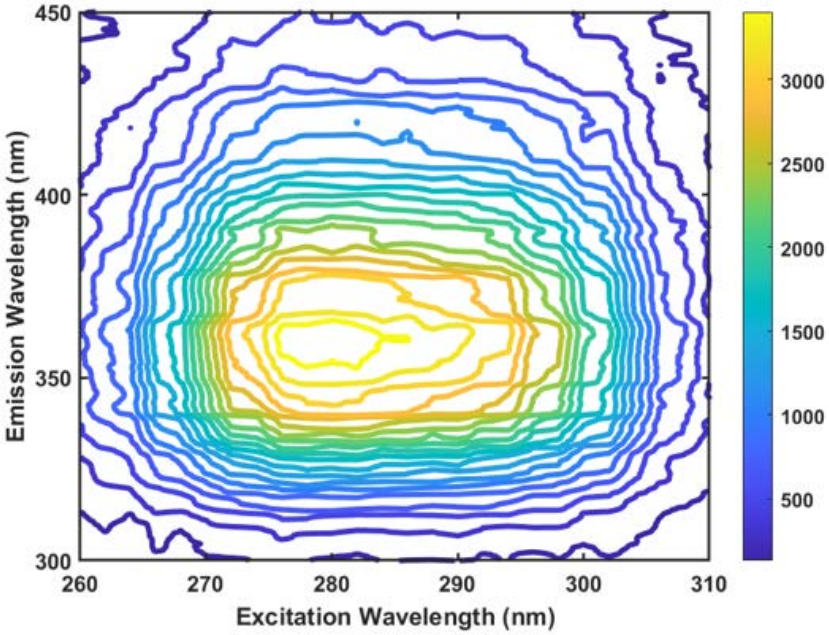

Figure 37: 2D contour plot of EEM for tryptophan (≈ 1 mg/mL) acquired over an excitation range of 260 to 310 nm in 2 nm steps.

Figure 36 and Figure 37 offer a detailed characterization of the fluorescence bands associated with tyrosine and tryptophan. In particular, while both amino acids absorb light at an excitation wavelength of $\lambda_{EX} \approx 280$ nm, the fluorescence band maximum occurs at a distinctly higher wavelength and intensity for tryptophan.

After acquiring these EEMs, a mixture of tyrosine and tryptophan (≈ 1 mg/mL concentration for each component) was created. The resulting EEM and synchronous fluorescence spectra are shown in Figure 38 and Figure 39 below.

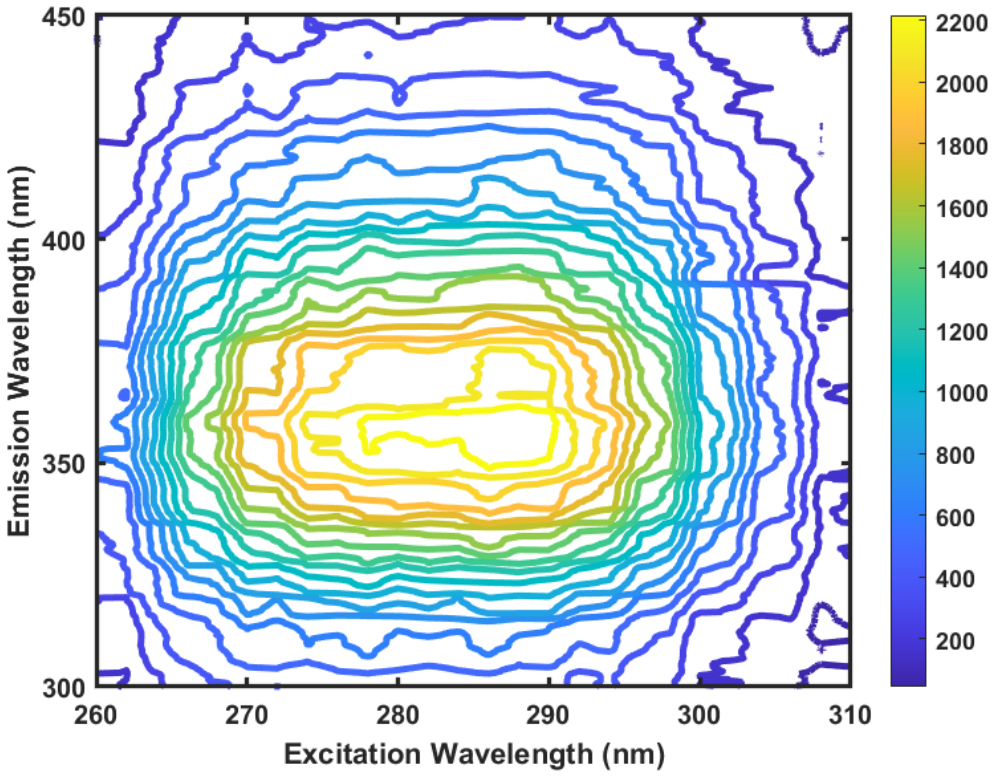

Figure 38: 2D contour plot of EEM for mixture of tyrosine and tryptophan (≈ 1 mg/mL concentration for each component) acquired over an excitation range of 260 to 310 nm in 2 nm steps.

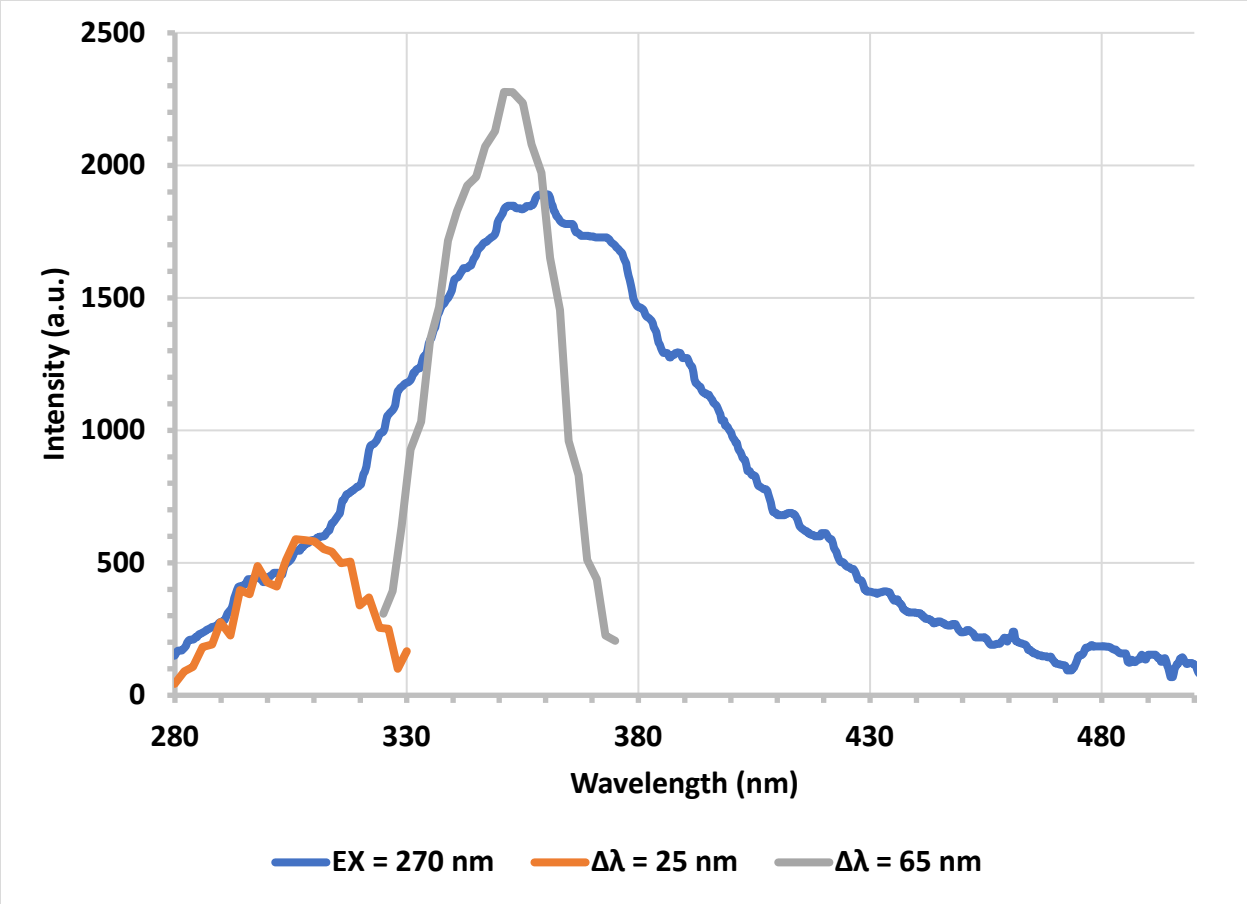

Figure 39: Normal fluorescence and synchronous fluorescence spectra of tyrosine and tryptophan mixture extracted from EEM.

Figure 39 demonstrates the utility of synchronous fluorescence in resolving the fluorescence bands of individual components within a mixture. Namely, the normal fluorescence spectrum is simply a broad, structureless band that cannot be uniquely assigned to either tryptophan or tyrosine individually. In contrast, the synchronous fluorescence spectra at $\Delta\lambda = 25$ nm and $\Delta\lambda = 65$ nm resolve the tyrosine and tryptophan components, respectively.

To further validate this procedure, the EEM and synchronous fluorescence spectra of *E. coli* bacteria were acquired. The synchronous fluorescence spectra were then compared with those acquired on a benchtop, commercial spectrometer (Shimadzu RF5301PC).

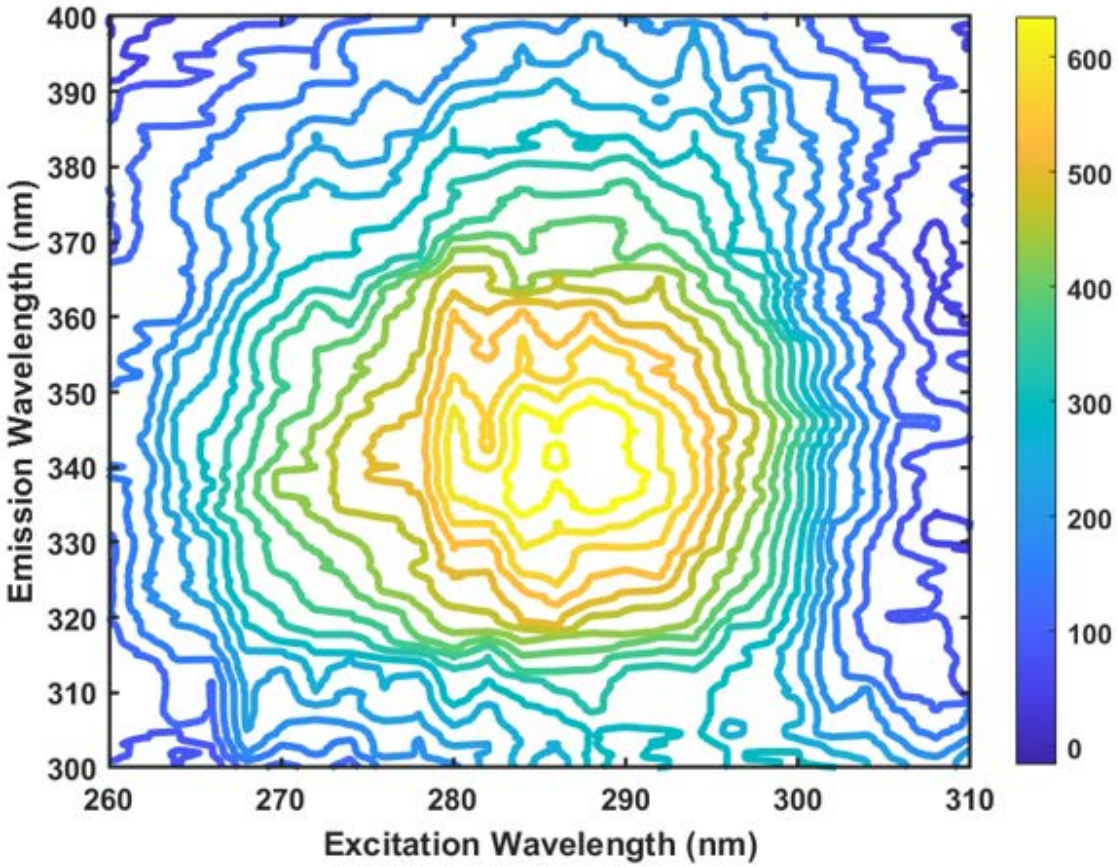

Figure 40: 2D contour plot of EEM for *E. coli* bacteria (≈ 10^8 cells/mL) acquired over an excitation range of 260 to 310 nm in 2 nm steps.

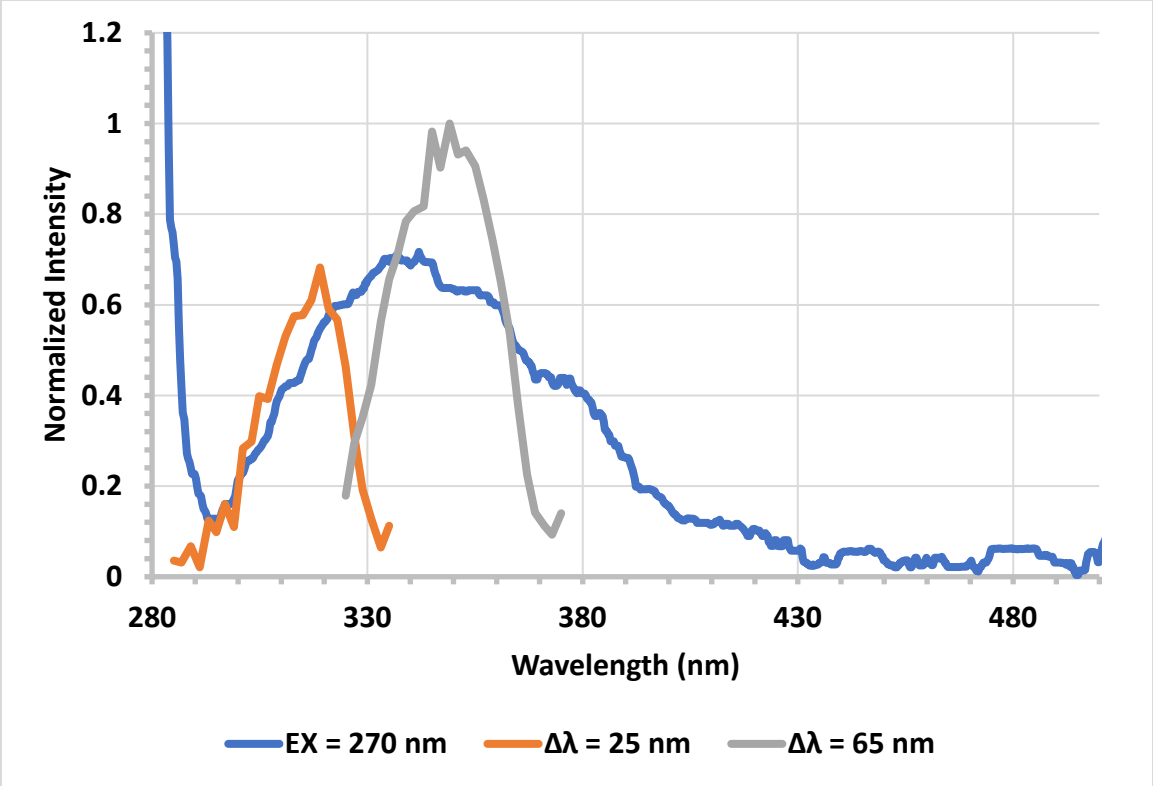

Figure 41: Normal fluorescence and synchronous fluorescence spectra of *E. coli* bacteria extracted from EEM. The spectra are normalized.

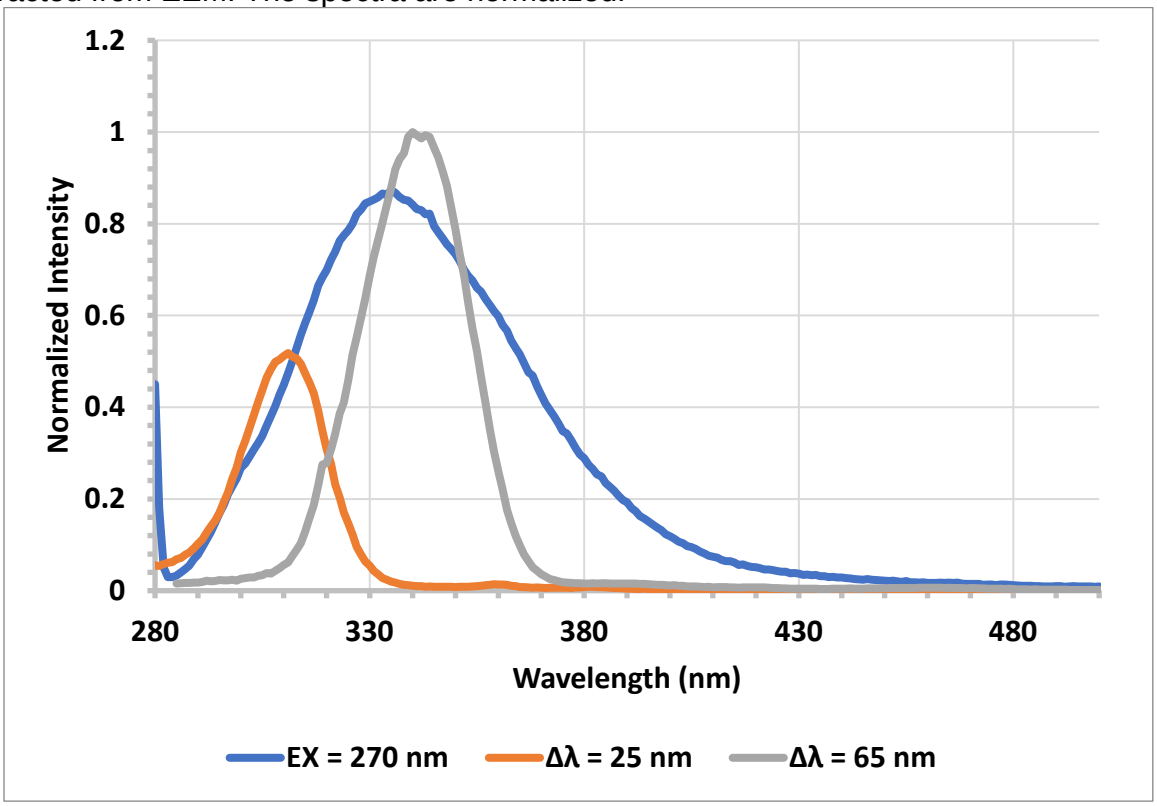

Figure 42: Normal fluorescence and synchronous fluorescence spectra of *E. coli* bacteria recorded with benchtop, commercial spectrometer. The spectra are normalized.

The portable and benchtop spectra are plotted in normalized units. In general, the agreement between the two set of spectra is very good, indicating that the components and techniques utilized in the portable instrument for acquiring synchronous spectra are validated. It is worthy to mention that the exact intensities and locations of certain bands may be slightly different due to variations in the detector sensitivity and excitation source intensity. For example, the benchtop instrument utilizes a Xenon lamp as its excitation source, which has a much broader output spectrum than the UV LED source in the portable instrument; this accounts for the difference in the range of the synchronous spectra and would also introduce variations in the source intensity. The detector used in the benchtop instrument, a photomultiplier tube (PMT), also possesses its own sensitivity curve which would differ from the linear image sensor used in the portable instrument. Nonetheless, the individual fluorescence bands of tyrosine and tryptophan, in both a mixture and bacteria, are successfully resolved through the synchronous fluorescence technique, thus validating the excitation monochromator subsystem.

4.4. Subsystem Conclusion

In conclusion, this subsystem satisfies all required functionalities. In particular, it is capable of serving as a scanning excitation source for acquiring the EEM of a sample and extracting synchronous fluorescence spectra. These capabilities were validated for *E. coli* bacteria and its cellular components, tryptophan and tyrosine. For next semester, additional UV excitation sources will be investigated to increase the output power of the excitation monochromator and sensitivity of the overall system.

5. Emission Monochromator Subsystem Report

5.1. Subsystem Introduction

The emission monochromator subsystem serves as the imaging spectrometer for detecting and recording the fluorescence spectra of bacteria under either fixed or scanning excitation. The subsystem is composed of a (1) optical bench with mirrors and a diffraction grating, (2) linear charge-coupled device (CCD) detector array, and (3) control electronics for digitizing the spectral data and communicating with the control and display unit subsystem. Commands are issued to this subsystem through a serial communication link between the computer and controller. These components are housed in a lightweight, portable enclosure.

5.2. Subsystem Details

5.2.1. Components

A picture of the current embodiment for the emission monochromator subsystem, along with its major components, is shown in Figure 43 below.

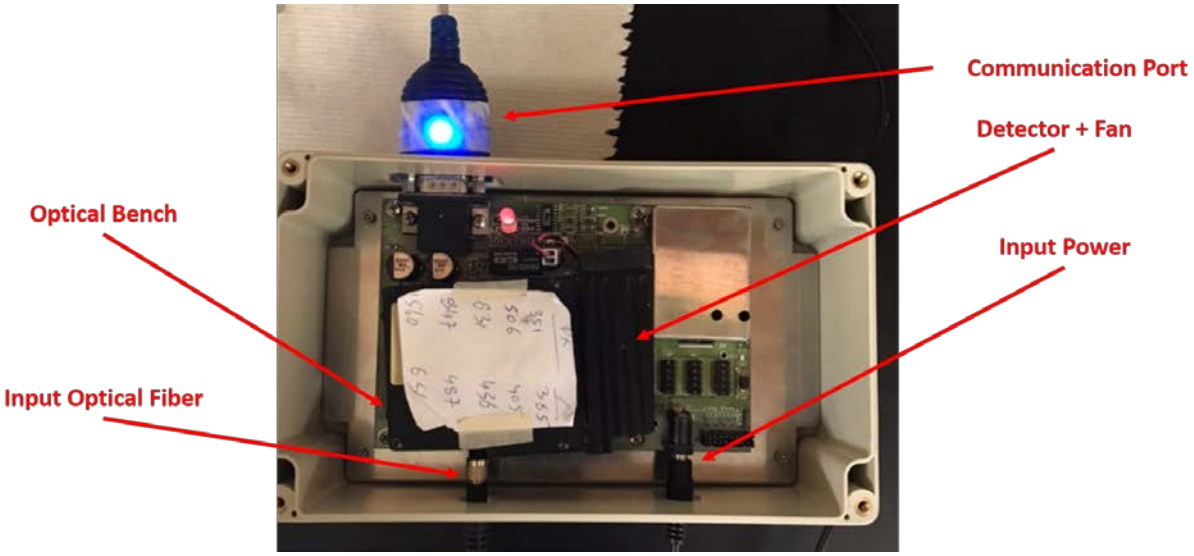

Figure 43: Emission monochromator subsystem and its major components.

The emission monochromator subsystem is an off-the-shelf spectrometer (BTC110-S) from B&W Tek. As shown in Figure 43, this system already includes an optical bench, input fiber port, input power port, detector and cooling fan, and communication port for setting acquisition parameters and acquiring spectral data. The optical bench itself is easily configurable and was modified with optical components, namely mirrors and a diffraction grating, with high efficiency in the UV region to increase the spectrometer's sensitivity to bacterial fluorescence. Details regarding the communication with the BTC110-S, and the associated procedures for setting acquisition parameters and receiving spectral data, were provided in the control and display unit subsystem report.

A mounting plate for this subsystem was designed and fabricated through the Physics Machine Shop at Texas A&M University with the assistance of Mr. Garrick Garza. A cheap, compact electronics project box was utilized as the enclosure. A picture of the overall design is shown in Figure 44 below.

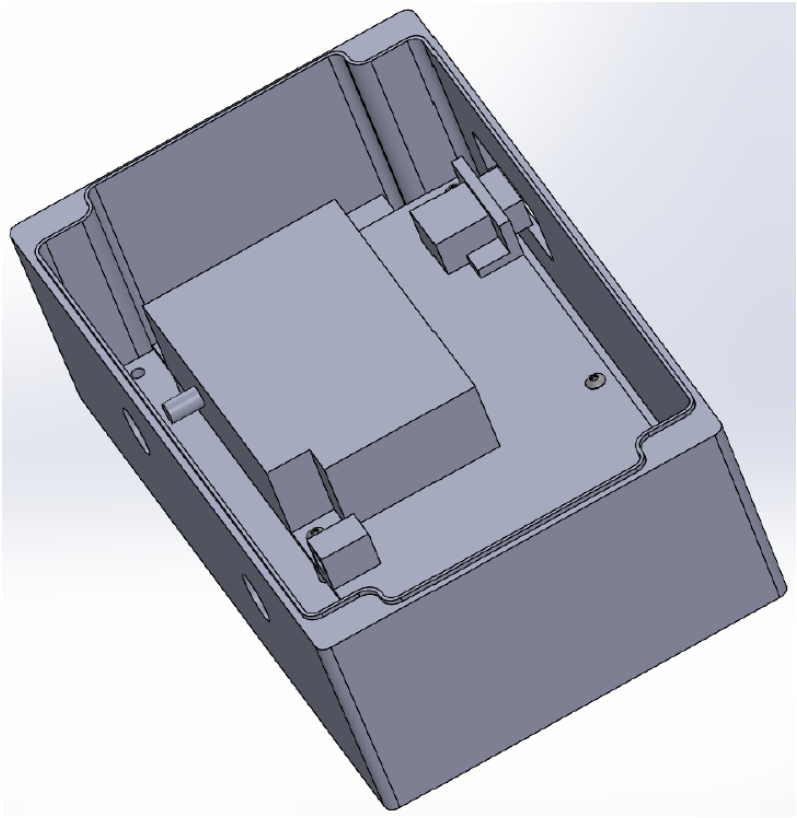

Figure 44: Design for the emission monochromator subsystem, including the enclosure and mounting plate.

5.2.2. Optical Bench

The design of the optical bench, namely its optical components, is critical in determining the sensitivity of the spectrometer in the UV region. The components of the optical bench are shown in Figure 45 below.

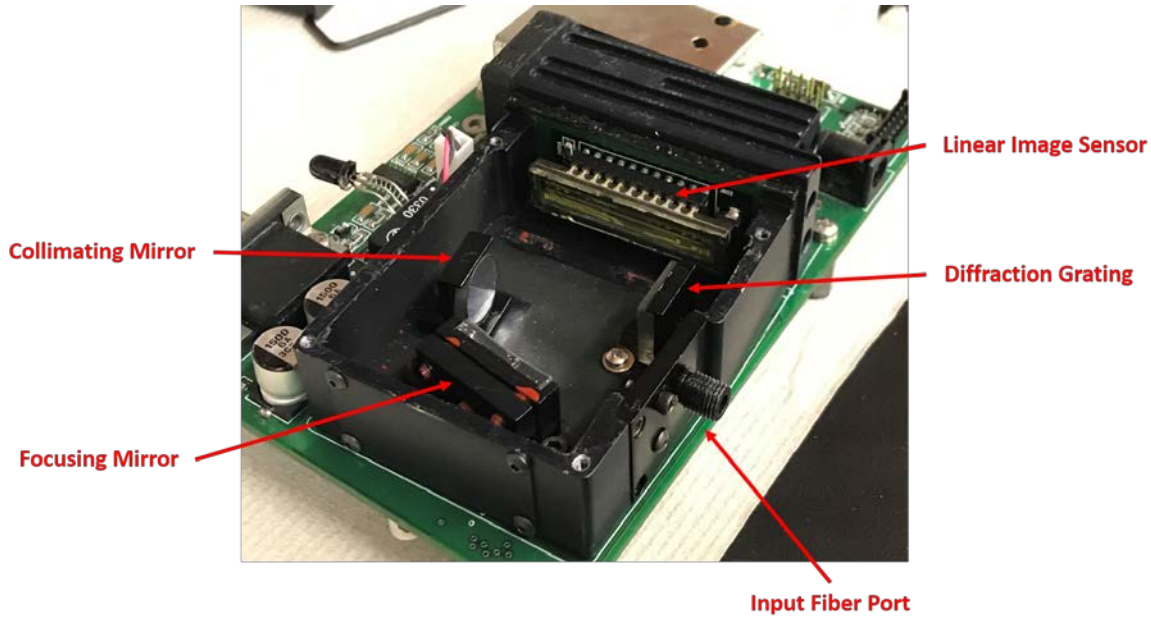

Figure 45: Optical bench and its major components.

Briefly, fluorescence entering the input fiber port will be collected and collimated by the collimating mirror, dispersed by the diffraction grating, and then focused onto the pixels of the linear image sensor, whereupon the spectrum will be digitized, stored, and transmitted to the computer. To achieve this, the optical bench had to be properly aligned to maximize the intensity of light falling onto the detector pixels. This was accomplished by performing horizontal and vertical adjustments on the mirrors and grating through the set screws in the optical bench. Such a process is depicted in Figure 46 below.

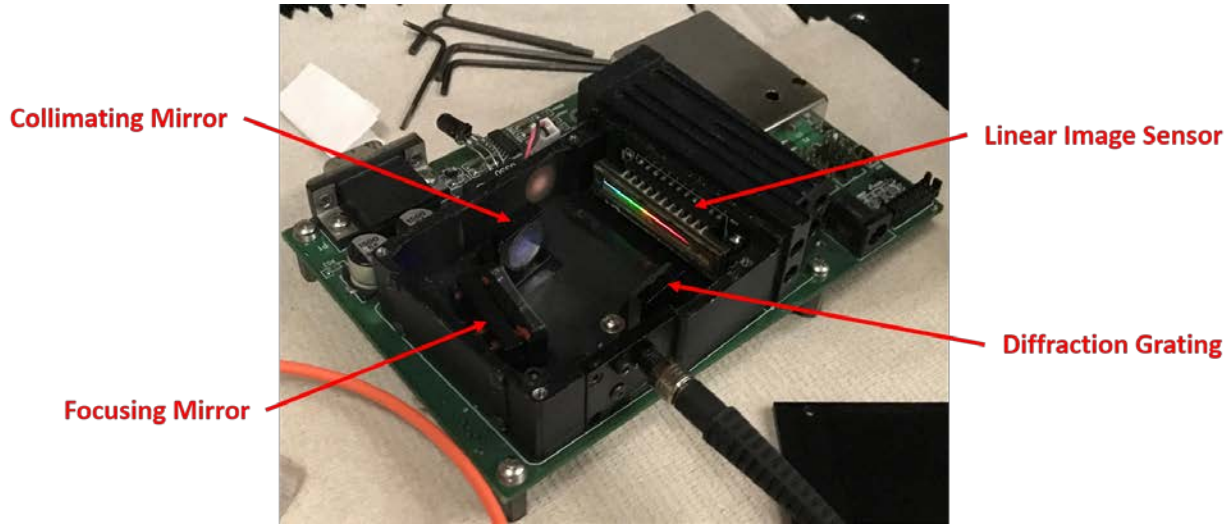

Figure 46: Optical bench during alignment process.

To increase the UV sensitivity of the spectrometer, the diffraction grating provided by B&W Tek was replaced with a UV diffraction grating possessing very high diffraction efficiency in the UV region (Newport Corporation 33025FL01-060R). The usage of this grating ensures that the fluorescence of bacteria and its components will not be significantly attenuated within the optical bench. The efficiency curve of this diffraction grating is provided in Figure 47 below and can be found to be as high as 75% in the UV region.

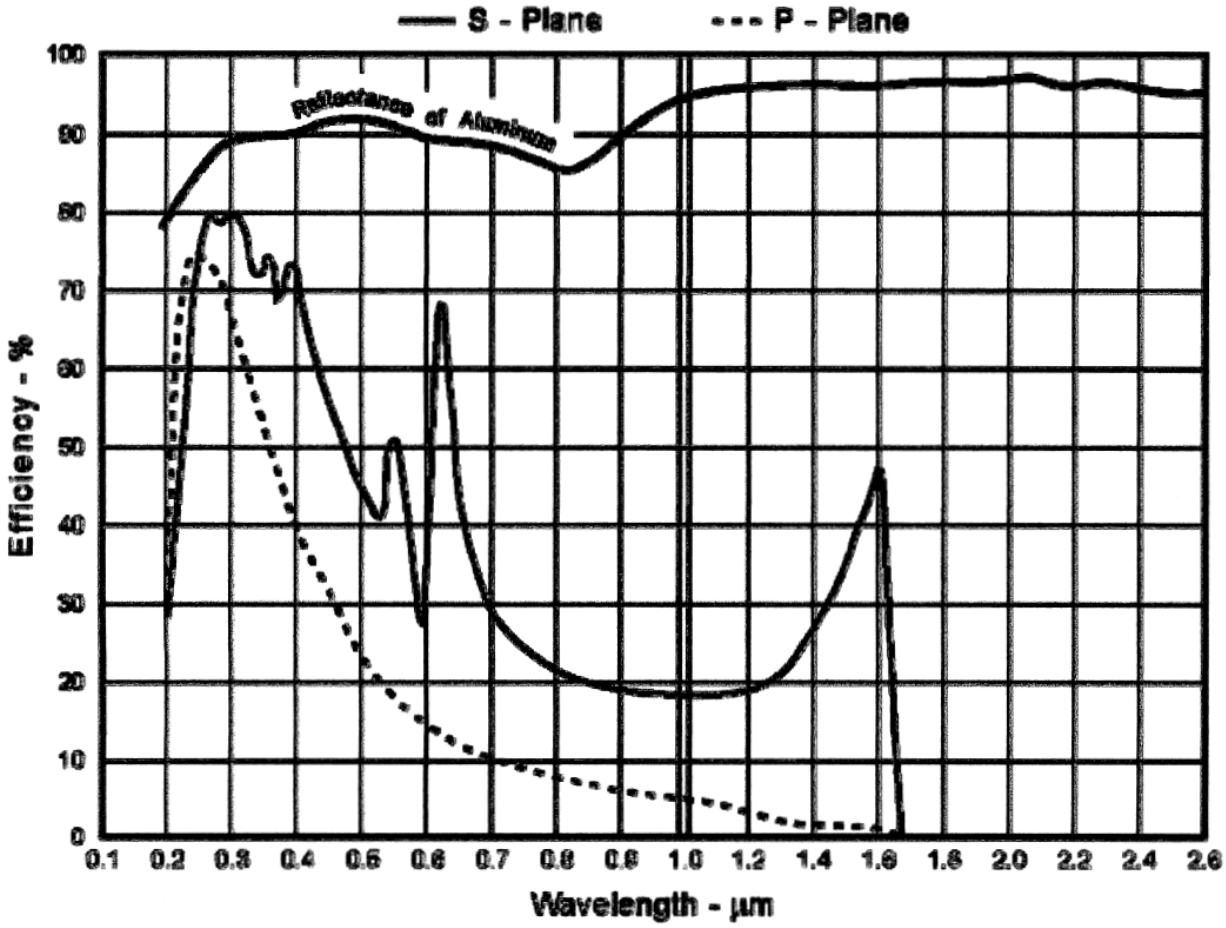

Figure 47: Diffraction grating efficiency curve [10].

In addition to the diffraction grating, the collimating mirror was replaced with a UV-enhanced mirror of the same size to further increase the efficiency of the spectrometer in the UV region.

5.2.3. Detector

The detector which is included in the BTC-110S is the Sony ILX511B linear image sensor, which is a CCD detector with 2048 pixels. This sensor natively has a very high sensitivity in the visible region, but poor sensitivity in the UV region. Therefore, this sensor was ordered with an additional dye coating known as Lumogen F Violet 570. This dye absorbs strongly in the UV region and fluoresces in the visible region, thereby increasing the UV sensitivity of the detector. This was another modification made to the optical bench in order to increase its UV sensitivity.

5.2.4. Operation

To utilize the spectrometer, it must first be calibrated. Calibration is performed by taking a source with known emission lines at distinct wavelengths, recording the spectrum, and deriving a fitting which provides the wavelength as a function of the detector pixel. This calibration is then utilized, in software, to convert the pixel-dependent intensity read out by the detector into a wavelength-dependent spectrum. A rather simple source to use in this process is the mercury-vapor lamp, also known as the compact fluorescent lamp (CFL), which is the same lamp typically used for overhead lighting in rooms within a building, for example. Figure 48 provides the well-known CFL spectrum, which possesses many distinct emission lines, while Figure 49 shows the CFL spectrum recorded by the emission monochromator.

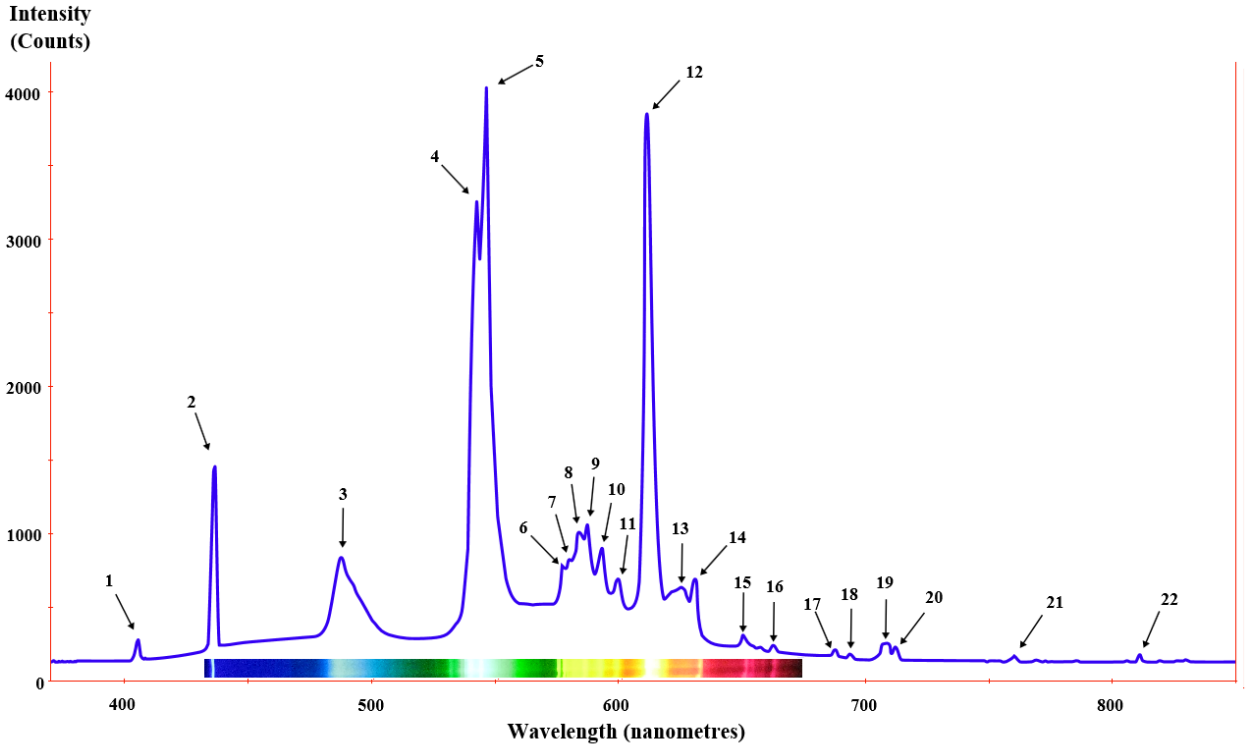

Figure 48: CFL (mercury-vapor lamp) spectrum [11].

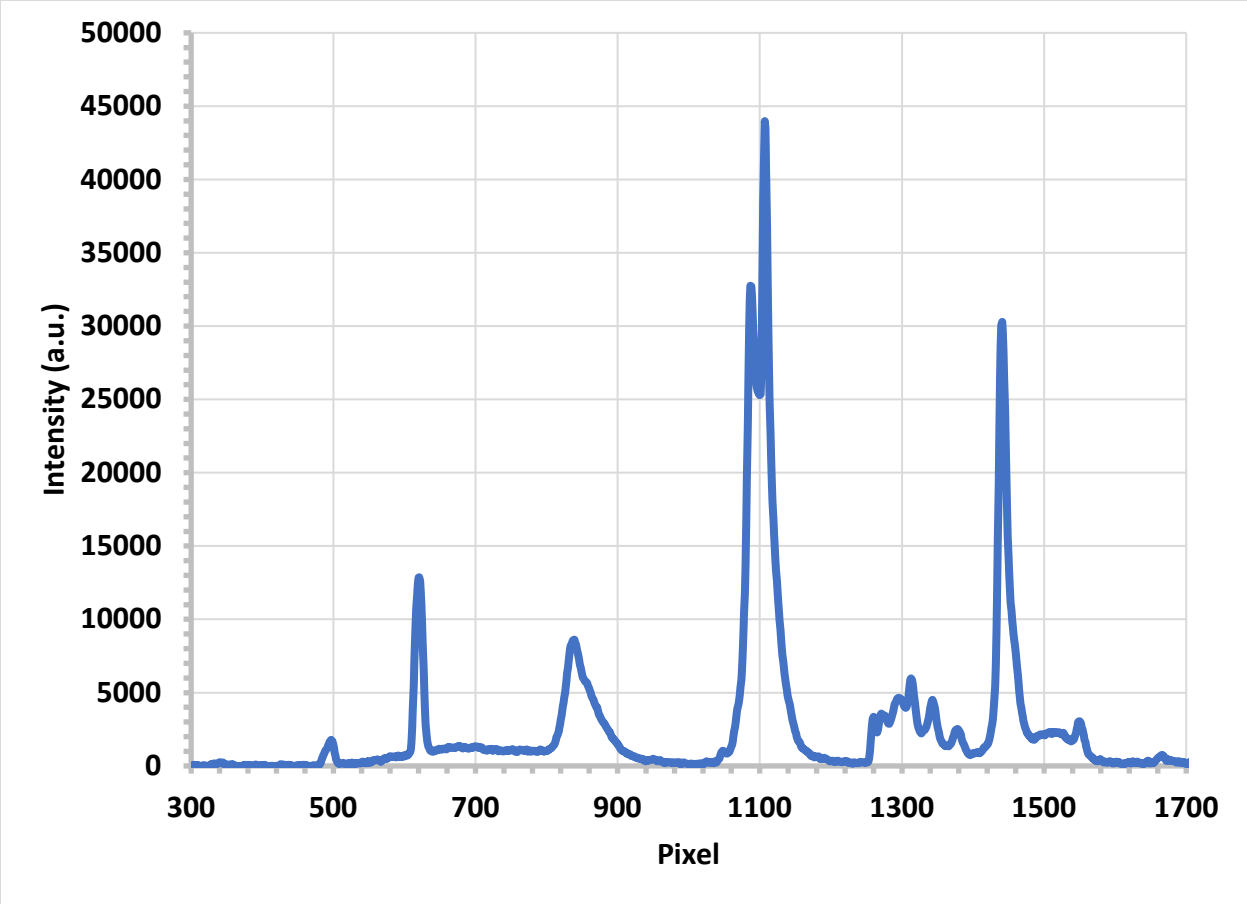

Figure 49: CFL (mercury-vapor lamp) spectrum recorded by the emission monochromator as a function of pixel.

From Figure 48 and Figure 49, distinct emission lines of the CFL spectrum could be identified at certain pixels. The resulting pixel-wavelength pairs were utilized to derive a second-order polynomial using the least squares method. This fitting accounts for slight nonlinearities along the focal plane within the spectrometer, although the relation is expected to be highly linear in general. Table 8 provides the pixel-wavelength pairs utilized in deriving this fitting.

Pixel	Wavelength (nm)
351	365
506	405
631	436
847	487
1560	651

Table 8: Pixel-wavelength pairs for calibrating spectrometer.

Figure 50 shows the resulting fitting which is derived from the measurements of the CFL spectrum.

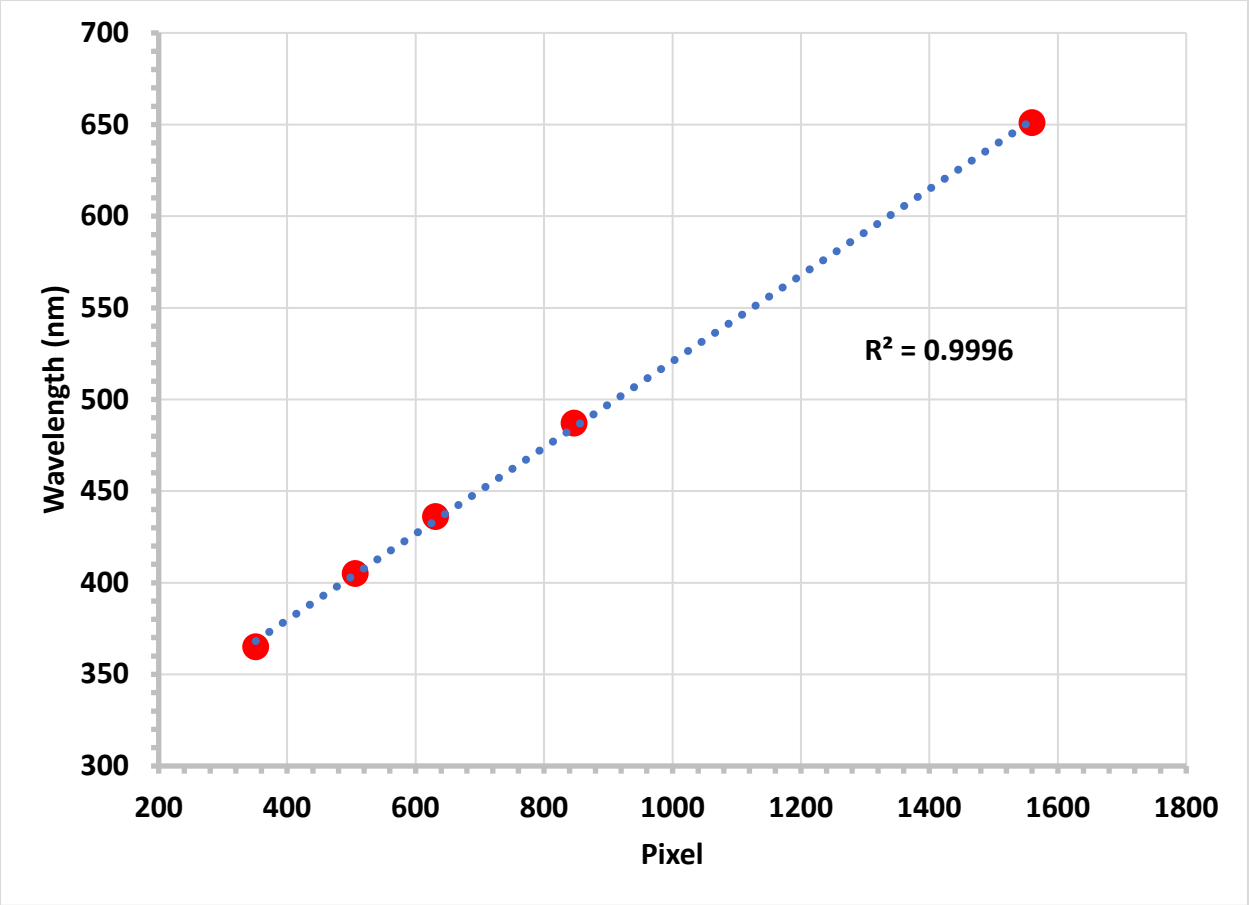

Figure 50: Calibration of emission monochromator subsystem by fitting the pixel-wavelength pairs of the CFL spectrum.

Power was supplied to the emission monochromator subsystem through its input power port, which simply requires a 5 V DC source.

5.3. Subsystem Validation

5.3.1. Normal Fluorescence Spectra of Bacteria Components

The UV sensitivity and calibration of the emission monochromator subsystem was first validated by recording the normal fluorescence spectra of tryptophan and tyrosine. The excitation source for these spectra was the disinfection unit. These spectra were compared against those recorded by a benchtop, commercial spectrometer (Shimadzu RF5301PC) for validation.

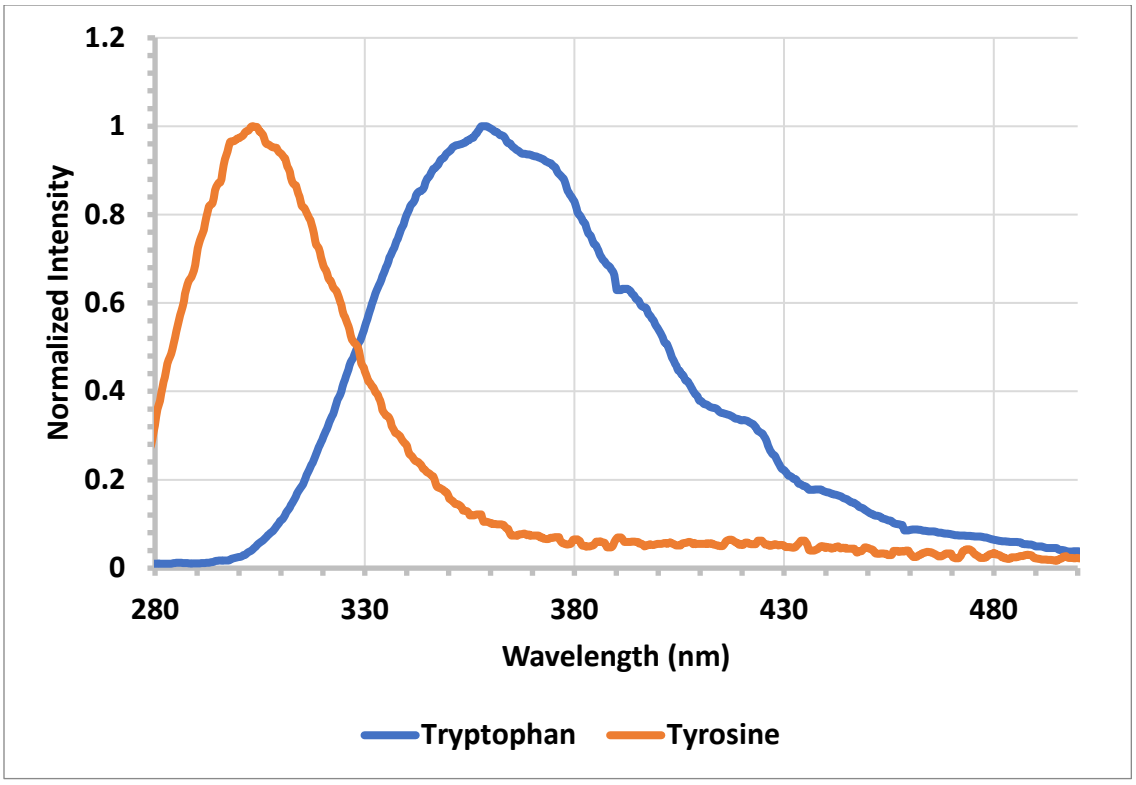

Figure 51: Normal fluorescence spectra ($\lambda_{EX} \approx 285$ nm) of tryptophan and tyrosine recorded by the portable spectrometer. The spectra are normalized.

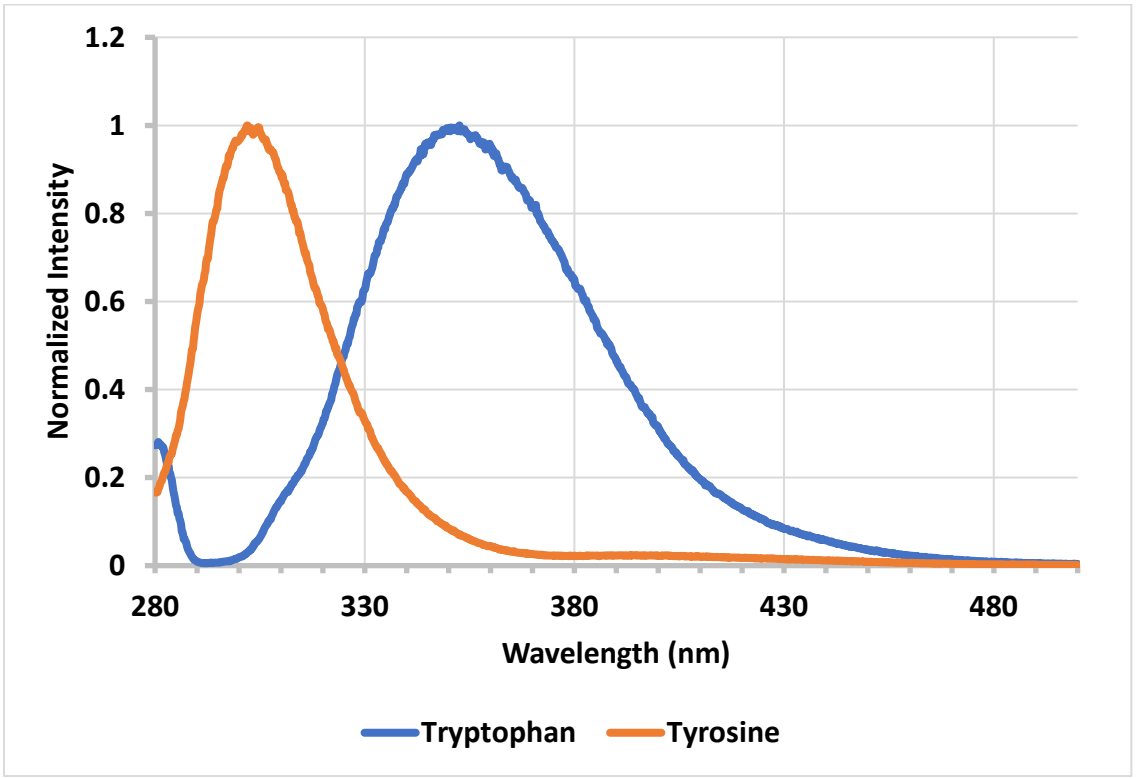

Figure 52: Normal fluorescence spectra ($\lambda_{EX} \approx 285$ nm) of tryptophan and tyrosine recorded by the benchtop spectrometer. The spectra are normalized.

The portable and benchtop spectra are plotted in normalized units. In general, the agreement between the two set of spectra is very good, indicating the spectrometer calibration was sufficiently performed. It can be noted that the resolution and signal-to-noise ratio (SNR) of the portable spectrometer are worse compared to those for the benchtop spectrometer, but that is expected.

5.3.2. Normal Fluorescence Spectra of *E. coli* Bacteria

The UV sensitivity and calibration of the emission monochromator subsystem was further validated by recording the normal fluorescence spectra of *E. coli* bacteria. The excitation source for these spectra was the disinfection unit. These spectra were again compared against those recorded by a benchtop, commercial spectrometer (Shimadzu RF5301PC) for validation.

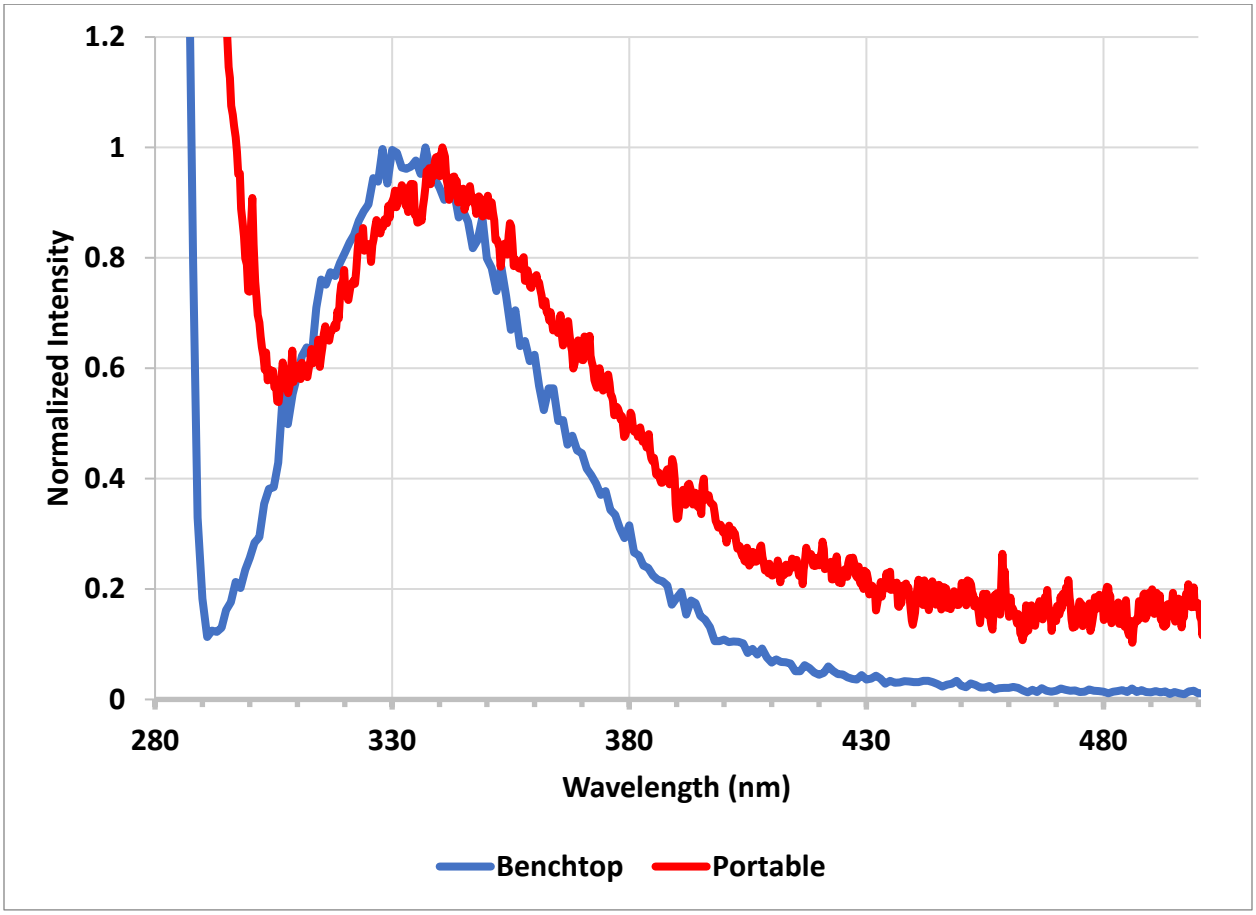

Figure 53: Normal fluorescence spectra ($\lambda_{EX} \approx 285$ nm) of *E. coli* bacteria recorded by the portable spectrometer. The spectra are normalized.

The portable and benchtop spectra are plotted in normalized units. In general, the agreement between the two set of spectra is very good, indicating the spectrometer calibration was sufficiently performed. It can be noted that the resolution and signal-to-noise ratio (SNR) of the portable spectrometer are worse compared to those for the benchtop spectrometer, but that is expected. This is also a validation of the spectrometer's enhanced UV sensitivity for bacterial detection.

During this subsystem testing, it was found that the CCD noise could become particularly prevalent in the acquired fluorescence spectra when the emission monochromator was on for long periods of time. To that effect, consider the fluorescence decay plot provided in Figure 54 below.

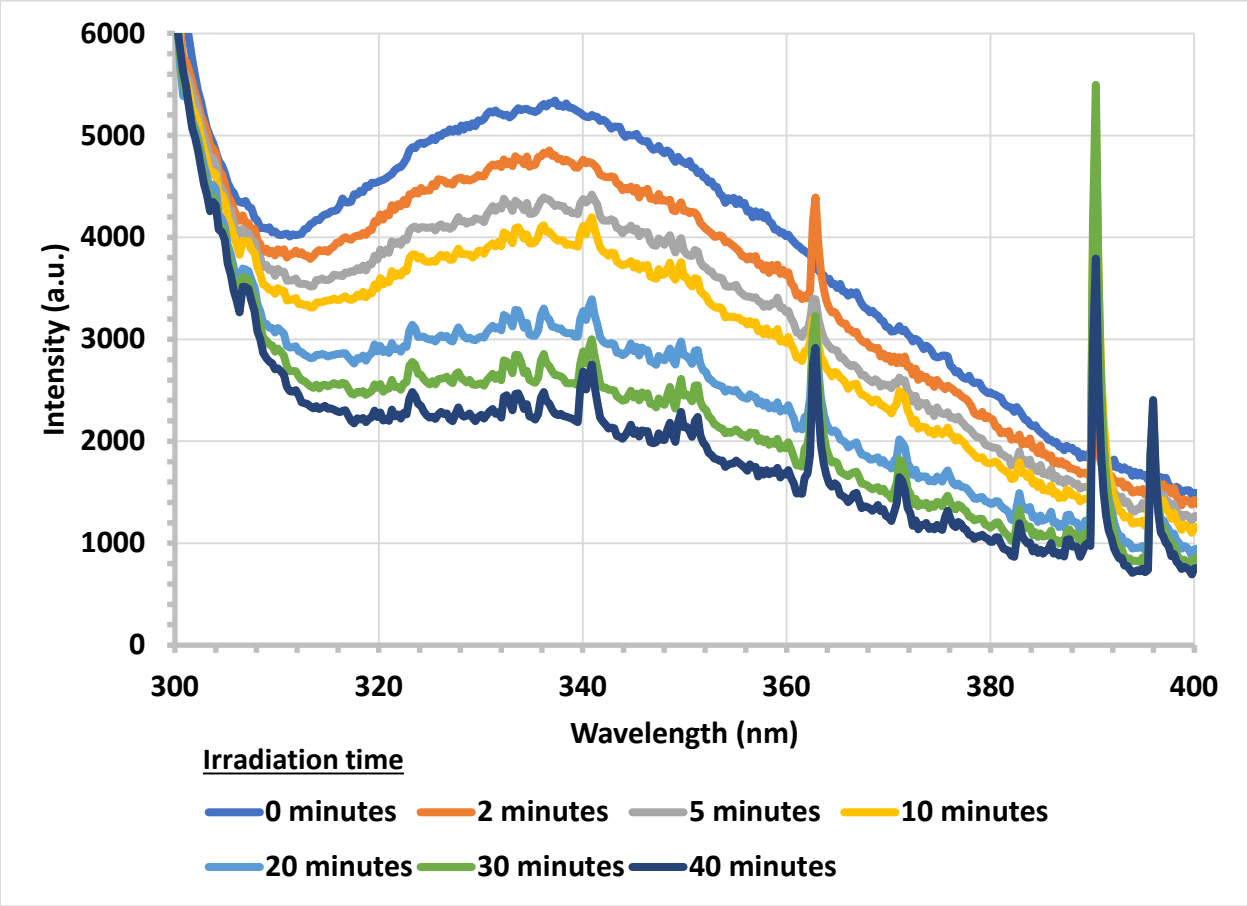

Figure 54: Normal fluorescence ($\lambda_{EX} \approx 285$ nm) spectra of *E. coli* bacteria ($\approx 10^8$ cells/mL) as a function of disinfection time.

Clearly, the spikes in the spectra, which are essentially noise spikes in the CCD readout itself, increase as subsystem remains on for a longer period of time. These spikes may therefore be attributed to the heating of the detector. To correct these spikes, a median filter with a width of 20 points was applied to all spectra, resulting in the plot shown in Figure 55.

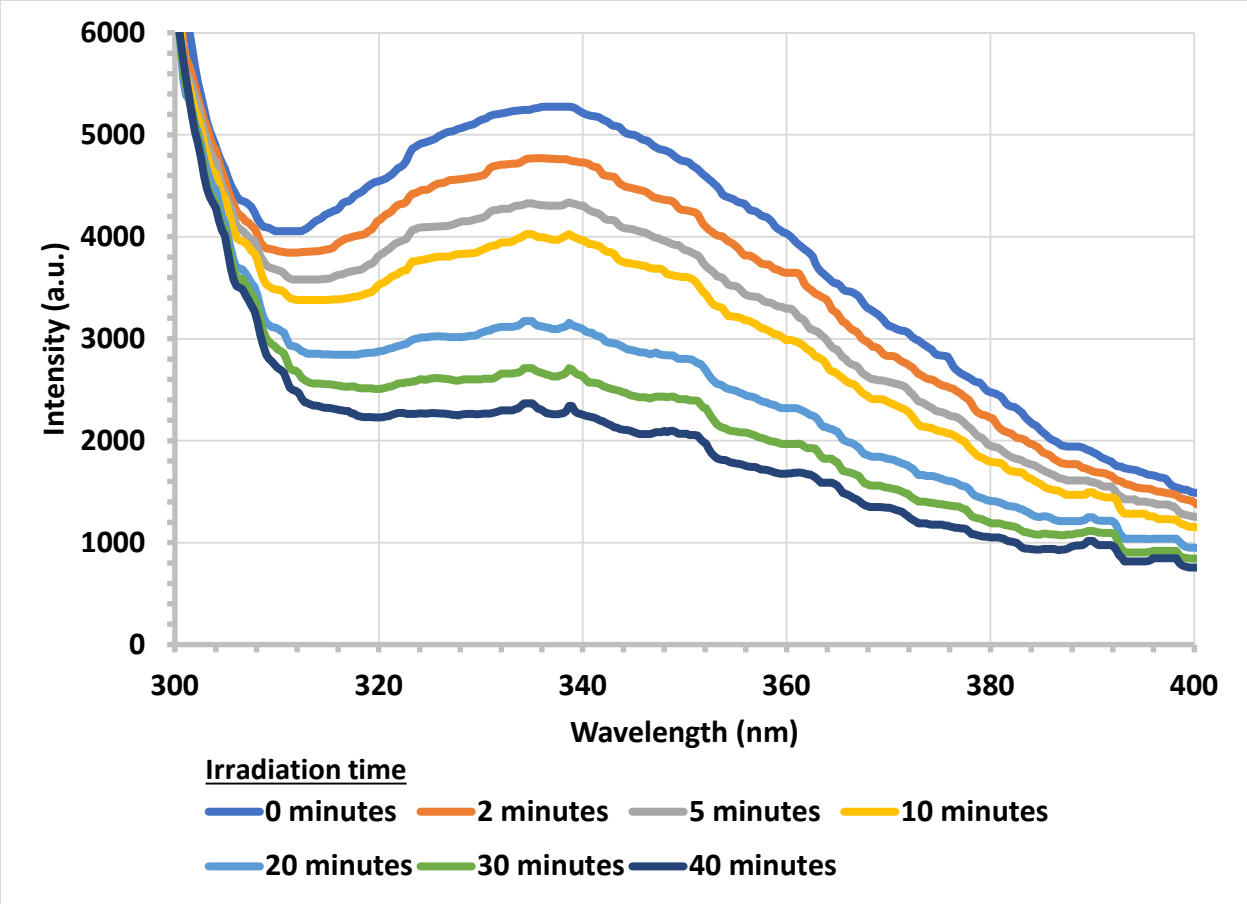

Figure 55: Normal fluorescence ($\lambda_{EX} \approx 285$ nm) spectra of *E. coli* bacteria ($\approx 10^8$ cells/mL) as a function of disinfection time with a median filter of width 20 points applied.

After applying a median filter, the spectra are significantly smoothened without any distortion occurring to the band shape or peak intensity. Median filtering is thus a rather useful technique in removing the CCD noise during spectral acquisitions. The effects of median filtering on the PCA clustering are quite dramatic as well, as shown in Figure 56 and Figure 57.

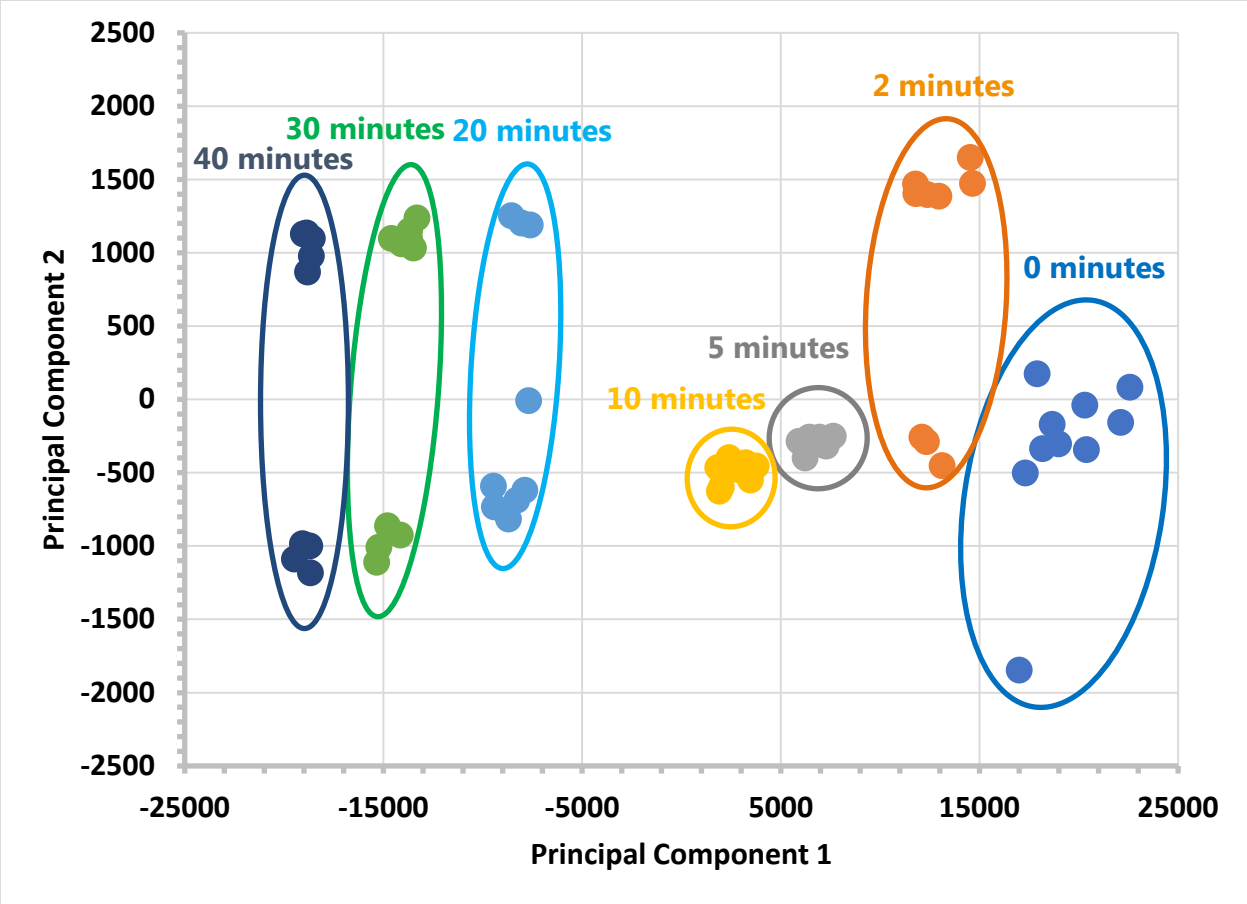

Figure 56: PCA score plot for UV irradiation experiment on *E. coli* bacteria ($\approx 10^8$ cells/mL) before performing median filtering.

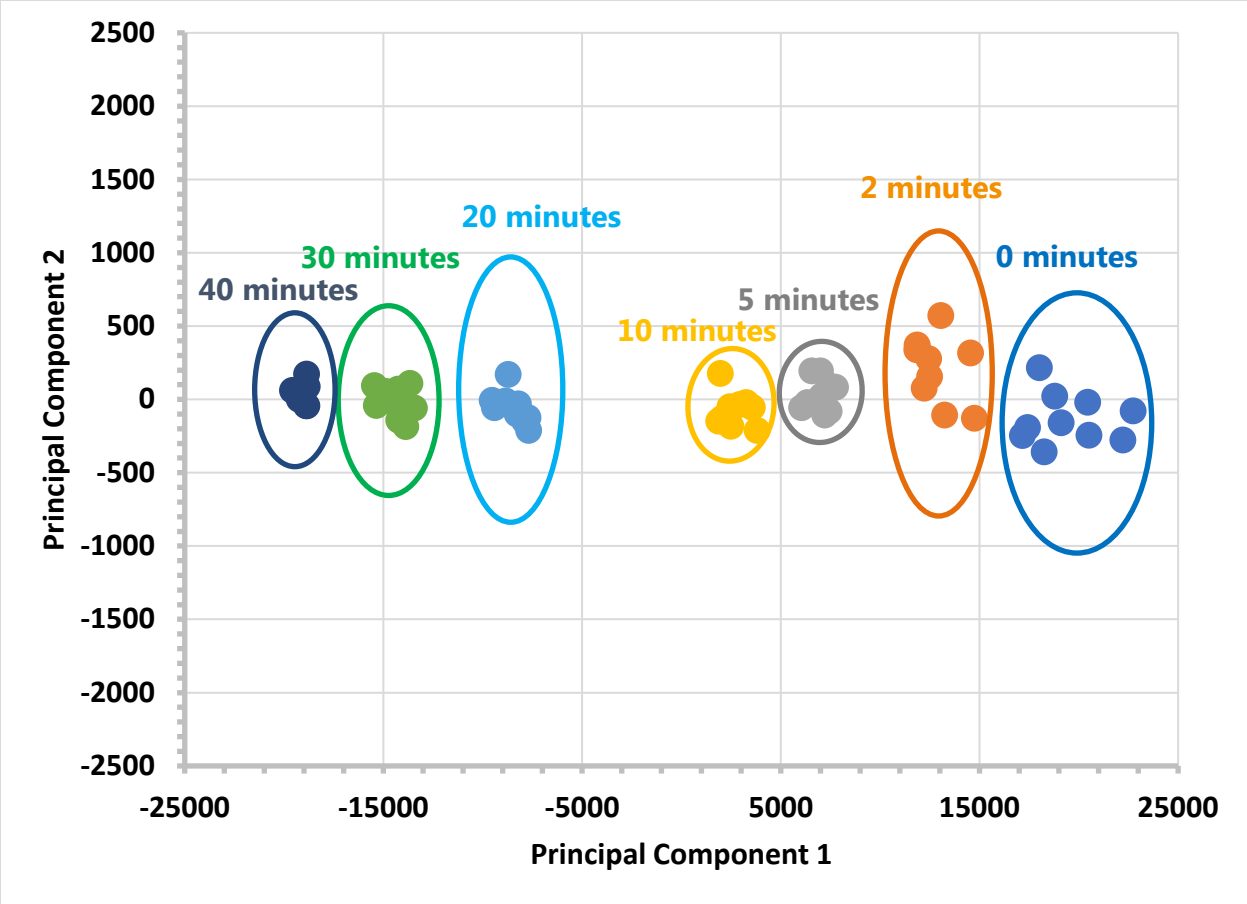

Figure 57: PCA score plot for UV irradiation experiment on *E. coli* bacteria (≈ 10^8 cells/mL) after performing median filtering.

Thus, median filtering provides a powerful means of improving the clustering in PCA score plots as well.

5.3.3. Operation with Disinfection Unit and Excitation Monochromator

The operation of the emission monochromator subsystem with the disinfection unit and excitation monochromator subsystems was already thoroughly discussed and validated. This validation includes the validation of the spectrometer's capability to record EEMs and synchronous fluorescence spectra.

5.4. Subsystem Conclusion

In conclusion, this subsystem satisfies all required functionalities. In particular, it possesses sufficient UV sensitivity for recording the fluorescence of bacteria components and bacteria itself. The calibration of the unit was validated as well. In regards to next semester, the sensitivity of the unit will continue to be optimized to achieve the smallest exposure times possible.

5.5. Citations

[1] DCB 241. (n.d.). Retrieved from http://stepcontrol.com/dc_dcb241/

[2] Spectrometer Command Set for BTC110/BRC100/BRC110/BTC200. (n.d.). Retrieved from http://www.bwtek.com

[3] Vo-Dinh T (1978) Multicomponent analysis by synchronous luminescence spectrometry. Anal Chem 50:396–401.

[4] Randive, R. (2016, March 1). Improved POU disinfection with UVC LEDs. Retrieved from https://www.watertechonline.com/improved-pou-disinfection-with-uvc-leds/

[5] Cantor CR, Schimmel PR (1980) Chapter 8: Other optical techniques. Biophysical Chemistry – Part 2: Techniques for the Study of Biological Structure and Function (W. H. Freeman and Company, New York), pp. 409–480.

[6] MTSM285UV-F1120S. (n.d.). Retrieved from http://marktechopto.com

[7] Li R, Goswami U, King M, Chen J, Cesario TC, Rentzepis PM (2018) In situ detection of live-to-dead bacteria ratio after inactivation by means of synchronous fluorescence and PCA. Proc Natl Acad Sci 115:668–673.

[8] RVXP4-280-SM-077132. (n.d.). Retrieved from https://rayvio.com/xpseries/

[9] Mini-Chrom Monochromators & Accessories. (n.d.). Retrieved from https://www.dynasil.com/knowledge-base/mini-chrom-monochromators/

[10] Efficiency Curve 060R. (n.d.). Retrieved from https://www.newport.com/p/33025FL01-060R

[11] Spectrum of Fluorescent Light. (n.d.). Retrieved from http://www.bealecorner.org/best/measure/cf-spectrum/